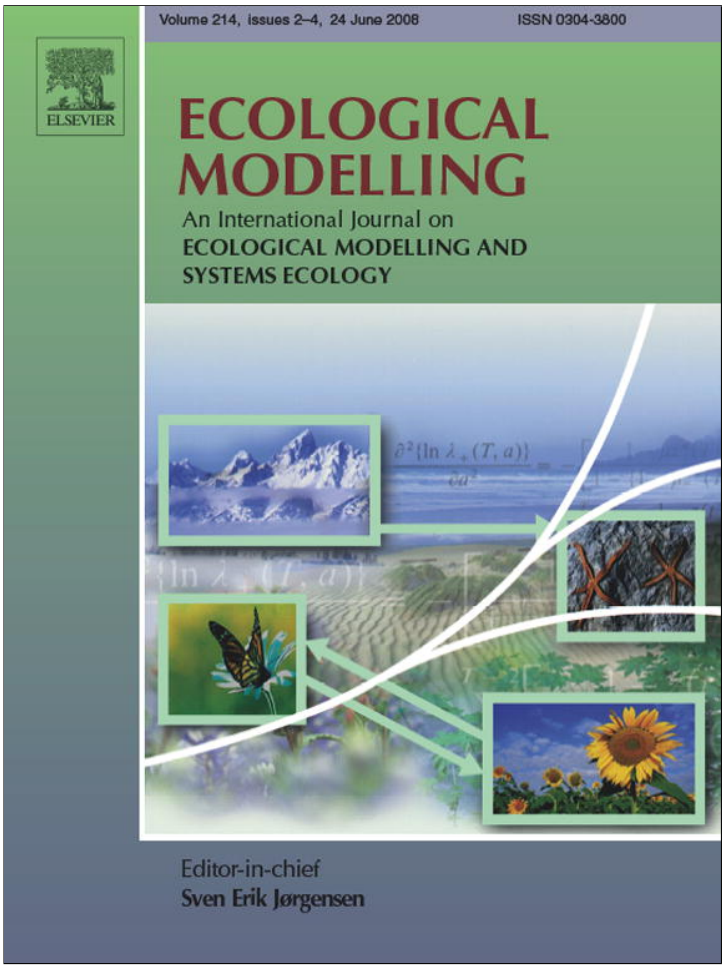

ECOLOGICAL MODELLING 214 (2008) 219–241

available at www.sciencedirect.com

ScienceDirect

journal homepage: www.elsevier.com/locate/ecolmodel

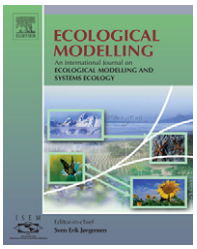

A two-dimensional ecological model of Lake Erie: Application to estimate dreissenid impacts on large lake plankton populations

Hongyan Zhang[a,*], *David A. Culver*[a], *Leon Boegman*[b]

[a] *Department of Evolution, Ecology, and Organismal Biology, The Ohio State University, Columbus, OH 43210 USA*
[b] *Department of Civil Engineering, Queen's University, Kingston, Ontario K71 3N6 Canada*

ARTICLE INFO

Article history:
Received 6 October 2007
Received in revised form
7 February 2008
Accepted 18 February 2008
Published on line 3 April 2008

Keywords:
Ecological model
Dreissena
Grazing impacts
Nutrient excretion

ABSTRACT

We constructed a complex ecological model of Lake Erie, EcoLE, based on a two-dimensional hydrodynamic and water quality model (CE-QUAL-W2). We used data from 1997 to calibrate the model, and data from 1998 and 1999 to verify it. The simulated surface and bottom water temperatures show good agreement with field observations. In spite of limitations of this 2D model and data availability, the simulated values of biological and nutrient state variables match well with field measurements. Although EcoLE's performance for the verification years is as good as that of the calibration year, the wide standard deviations of both field measurements and model simulations as well as the complexity of an ecosystem of this size make us consider our model more as a valid analytical tool rather than a predictive one at this moment. Nevertheless, we have constructed the first fine-scale dynamic ecological model of a large lake that couples hydrodynamics and detailed food web of lower trophic levels and is driven by real-time air temperature and wind conditions and the inputs from the atmosphere and tributaries. Using the model we investigate the impacts of zebra mussels (*Dreissena polymorpha*) and quagga mussels (*D. bugensis*) on phytoplankton of Lake Erie. The simulation results show that dreissenid grazing impacts on non-diatom edible algae (NDEA) are weakened by the boundary layer above the basin bottom. However, dreissenid grazing impacts on diatoms are less affected by the boundary layer due to the higher sinking rates of diatoms. Dreissenid mussels increase non-diatom inedible algae (NDIA) rapidly with increasing mussel population size, because the dreissenid population excretes a large amount of ammonia and phosphate. Our results indicate that dreissenid mussels have weak direct grazing impacts on algal biomass, while indirect effects of their nutrient excretion have a greater impact on the system.

1. Introduction

Lake Erie is the southernmost of the Laurentian Great Lakes, with its center at 42°15′ north latitudes and 81°15′ west longitudes, and its long axis at about N70°E. It is approximately 386 km (240 miles) long and more than 80 km (50 miles) wide at its midpoint (Fig. 1). Its watershed's relatively warm weather and high productivity attract more people than the other Great

* *Corresponding author. Current address*: Cooperative Institute for Limnology and Ecosystems Research, School of Natural Resources and Environment, University of Michigan, and Great Lakes Environmental Research Laboratory, National Oceanic and Atmospheric Administration, 2205 Commonwealth Boulevard, Ann Arbor, MI 48105, USA. Tel.: +1 734 741 2354; fax: +1 734 741 2095.
E-mail address: hongyanzhang302@yahoo.com (H. Zhang).
0304-3800/$ – see front matter © 2008 Elsevier B.V. All rights reserved.
doi:10.1016/j.ecolmodel.2008.02.005

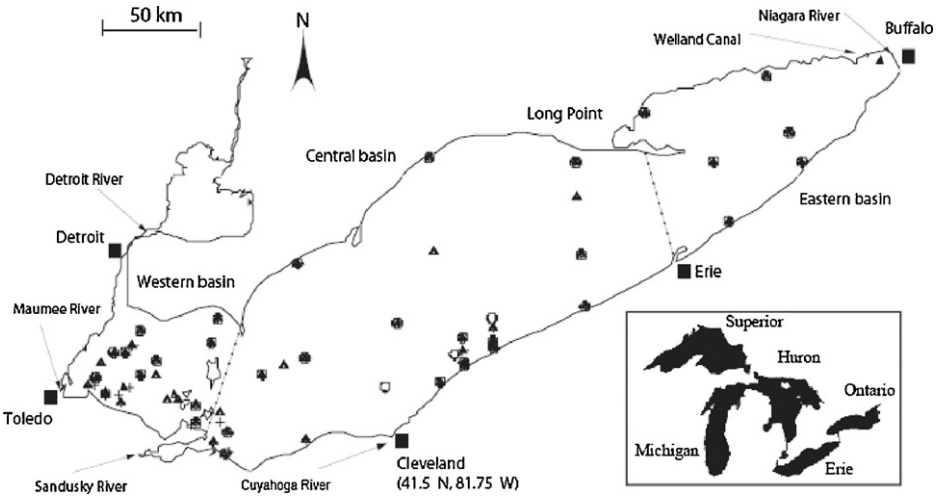

Fig. 1 – Lake Erie and its sampling sites (plus for 1997, triangle for 1998, circle for 1999).

Lakes, but its watershed's high human population has made it become increasingly a repository of municipal and industrial wastes, particularly prior to the 1970s. Fortunately, its water quality has been improved extensively since the phosphorus (P) reduction program (Great Lakes Water Quality Agreement, GLWQA) was implemented (Rockwell et al., 1989; Makarewicz and Bertram, 1991; Bertram, 1993; Leach, 1993; Krieger et al., 1996; Gopalan et al., 1998).

Lake Erie has become a classic and well-known case of successful eutrophication management, but the invasion of *Dreissena* spp. into Lake Erie from Europe complicates evaluation of the effectiveness of efforts to the P reduction program. Zebra mussels (*Dreissena polymorpha*) invaded Lake Erie in the late 1980s. Another exotic species, quagga mussels (*D. bugensis*), invaded in the early 1990s and are replacing zebra mussels and have become dominant in the central and eastern basins (May and Marsden, 1992; Mills et al., 1999; Jarvis et al., 2000). Although zebra and quagga mussels are different species, they have similar ecological impacts on Lake Erie. Although intensive studies have been carried out to investigate the structures and functions of ecosystems invaded by dreissenids, dreissenids' impacts on algae in the water column are still unclear because they consume phytoplankton from their position on the lake bottom. Early studies based on small-scale laboratory experiments tended to overestimate mussels' impacts (MacIsaac et al., 1992). Recent field experiments (Ackerman et al., 2001; Edwards et al., 2005; Boegman et al., 2008a) took hydrodynamics into account and showed that zebra mussels create a 1-m thick concentration boundary layer, which has a low phytoplankton biomass compared with the upper waters. Dreissenid impacts on waters in the upper, productive layers depend on the rate of delivery of algae to and from the boundary layer at the bottom. Not only do dreissenids affect water clarity near the bottom, they also affect algal succession by selective rejection of cyanobacteria (Vanderploeg et al., 2001) and by nutrient excretion resulting in lowered N:P ratios in the water column (Arnott and Vanni, 1996; Conroy et al., 2005a).

Previous Lake Erie models (Chapra, 1979; Vollenweider et al., 1979; Di Toro and Connolly, 1980; Lam et al., 1983) are too simple to analyze the present water quality situation. They have no (or very low) spatial resolutions. Moreover, none of these models include real-time meteorological conditions, and the physical mixing processes between spatial components were set as constants. Boegman et al.'s (2008a,b) model overcomes the above limitations. However, their model only includes one single algal group, and zooplankton is modeled as an external forcing function. A comprehensive ecological modeling incorporating both hydrodynamic and detailed food web models with fine spatial and temporal resolution is increasingly needed to investigate complicated ecosystem problems that Lake Erie is facing. For example, ecologists still cannot explain dreissenids' role in the recent increase in the frequency and magnitude of *Microcystis* blooms in recent years in Lake Erie (Vanderploeg et al., 2001; Vincent et al., 2004; Bierman et al., 2005; Conroy and Culver, 2005; Rinta-Kanto et al., 2005) or in the increase in the hypoxic area in the central basin during summer stratification.

In response to these needs, we have constructed a two-dimensional mathematical ecological model of Lake Erie, EcoLE, which includes physical, chemical and biological components. This model is based on Boegman et al.'s (2001, 2008a,b) hydrodynamic and water quality model, CE-QUAL-W2. We improve their model by separating algae into three groups and incorporating detailed zooplankton submodels (see Section 2). Thus, our model can be used for investigating ecosystem processes regarding algal succession, competition between mussels and zooplankton on food, importance of internal phosphorus loading relative to external phosphorus loading, and fish recruitment, etc. The physical environment in EcoLE is dynamically driven by daily meteorological data. The model's two dimensions (longitude and vertical) catch the main spatial characteristics that affect water quality management. For example, longitudinally, Lake Erie is eutrophic in the western basin and becomes less so eastwards. Vertically, Lake Erie has seasonal and diel thermostratification, whereas mussel populations create boundary layers at the bottom. Adding a third, latitudinal, dimension, surely would include additional phenomena, such as gyres, or the Maumee and Sandusky river plumes traveling along the southern shore, or concentration gradients of nutrients and plankton

between the nearshore and offshore zones. However, running three-dimensional models on a computer is very time consuming. For example, the three-dimensional GLCFS (Great Lakes Coastal Forecasting System) is run on a supercomputer, so one surely cannot finish a single run within 2 h on a desktop computer. Moreover, GLCFS is a purely physical model and at this point has no chemical or biological components at all. Nevertheless, given the rapid development in computational power, a three-dimensional model coupled with wetland models would be a logical next step. The three-dimensional hydrodynamic and water quality model ELCOM-CAEDYM is presently being developed for Lake Erie (Leon et al., 2006). Comparisons between different models and spatially/temporally limited field observations will all help us understand the complexity of Lake Erie.

After calibration and verification, we used EcoLE to test the effects of dreissenid mussel populations on algae. We hypothesize that dreissenids' grazing impacts on algal groups are highly constrained by the boundary layer above the mussel bed, so that even a large mussel population would not depress the phytoplankton community in Lake Erie. We also hypothesize that dreissenids' nutrient excretion has a greater role in algal succession than does their grazing, especially when the mussel population is large. To test these hypotheses, we simulate their basin-wide population grazing impacts on algae and basin-wide population nutrient excretion. Exploiting the flexibility of an ecological model, we varied mussel population sizes to investigate how mussel population changes affect algal community dynamics.

2. Model description

2.1. The physical model

CE-QUAL-W2 model (version 2.0), developed by US Army Corps of Engineers, is a two-dimensional, longitudinal/vertical, hydrodynamic and water quality model, which is constructed to simulate relatively long and narrow waterbodies exhibiting longitudinal and vertical water quality gradients (Cole and Buchak, 1995; Boegman et al., 2001). Hundreds of studies have applied this model to water bodies of various kinds (rivers, reservoirs, lakes and estuaries) all over the world (e.g., Palmieri and de Carvalho, 2006).

Boegman et al. (2001) modified CE-QUAL-W2 to simulate Lake Erie's hydrodynamics for 1994. They divided Lake Erie into as many as 65 vertical layers at 1 m intervals and 222 longitudinal segments from west to east. The depths of segments were assigned relative to the Great Lakes Datum (GLD) of 1985. A unique width was specified for each cell. Their model does a good job simulating water levels, water currents, and thermal stratification.

Our model, EcoLE, uses Boegman et al.'s modified CE-QUAL-W2 model to simulate the physical environment of Lake Erie with physical, chemical and biological input data from May to September seasons in 1997, 1998, and 1999. No changes in their model of the physical dynamics of the lake were made except for those parts related to short-wave solar radiation and wind. Boegman et al., used meteorological data measured from buoys on the lake in 1994 with solar radiation measured directly, whereas the meteorological data used in this paper are wind speed and direction, precipitation, air temperature, dew point, and cloud cover measurements taken every 3 h on land along the shoreline of Lake Erie (Toledo Express Airport, OH; Cleveland Hopkins International Airport, OH; Erie Terminal Building, PA; Greater Buffalo International Airport, NY) because no on-lake solar radiation data were available for 1997, 1998, or 1999. However, the original version of CE-QUAL-W2 (Cole and Buchak, 1995) uses meteorological data measured on land, and calculates solar radiation from solar altitude and azimuth, adjusted for cloud cover. Thus we adopted Cole and Buchak's (1995) codes for calculating solar radiation and infer the wind field over the lake from shore-based measurements.

2.2. The chemical–biological model

EcoLE divides the phytoplankton into three groups: non-diatom edible algae (NDEA), non-diatom inedible algae (NDIA), and diatoms (Fig. 2). New zooplankton (cladoceran and copepod) submodels are also included. Dreissenid mussels are included as external grazing and nutrient excretion forces (not as a state variable). The growing season is simulated from 10 May to 30 September of 1997, from 10 June to 30 October of 1998, and from 20 May to 29 September of 1999, reflecting the availability of field data for initialization, calibration, and validation of the model.

2.2.1. Phytoplankton

Phytoplankton is the primary producer and base of the food web in most freshwater systems. The algae edible or inedible by herbivorous zooplankton are defined as the Ohio State University's Lake Erie Plankton Abundance Study database (LEPAS) (Zhang, 2006). NDEA are dominated by *Chroomonas*, solitary green, *Cryptomonas*, *Rhodomonas*, *Dinobryon*, and *Chlamydomonas*. Diatoms are dominated by *Melosira*, *Fragilaria*, *Asterionella*, *Cyclotella*, and *Gyrosigma*. NDIA are dominated by the cyanobacterial genus *Microcystis*. Phytoplankton is simulated based on the conservation of mass, assuming that the only source of algae to the lake is through growth from photosynthesis in the model, as external algal loading data are unavailable. Algal growth is governed by temperature, light, and nutrients. This is briefly described below (for details, see Cole and Buchak, 1995 and Cole and Wells, 2003).

2.2.2. Phytoplankton temperature adjustment functions (λ_T)

We applied an asymmetric temperature function to simulate the influence of temperature on phytoplankton biological processes (Thornton and Lessem, 1978, see in Bowie et al., 1985; Cole and Buchak, 1995), which combines two logistic equations to describe the rising (γ_1) and falling (γ_2) limbs of the temperature optimum curve. Compared with most temperature functions with a single optimum temperature value, a no-growth low temperature (T_1) and a no-growth high temperature (T_4), the asymmetric temperature function allows an optimum temperature range (T_2–T_3). Diatoms tend to have a lower optimum temperature range, while blue-green algae tend to have a higher optimum temperature range than greens

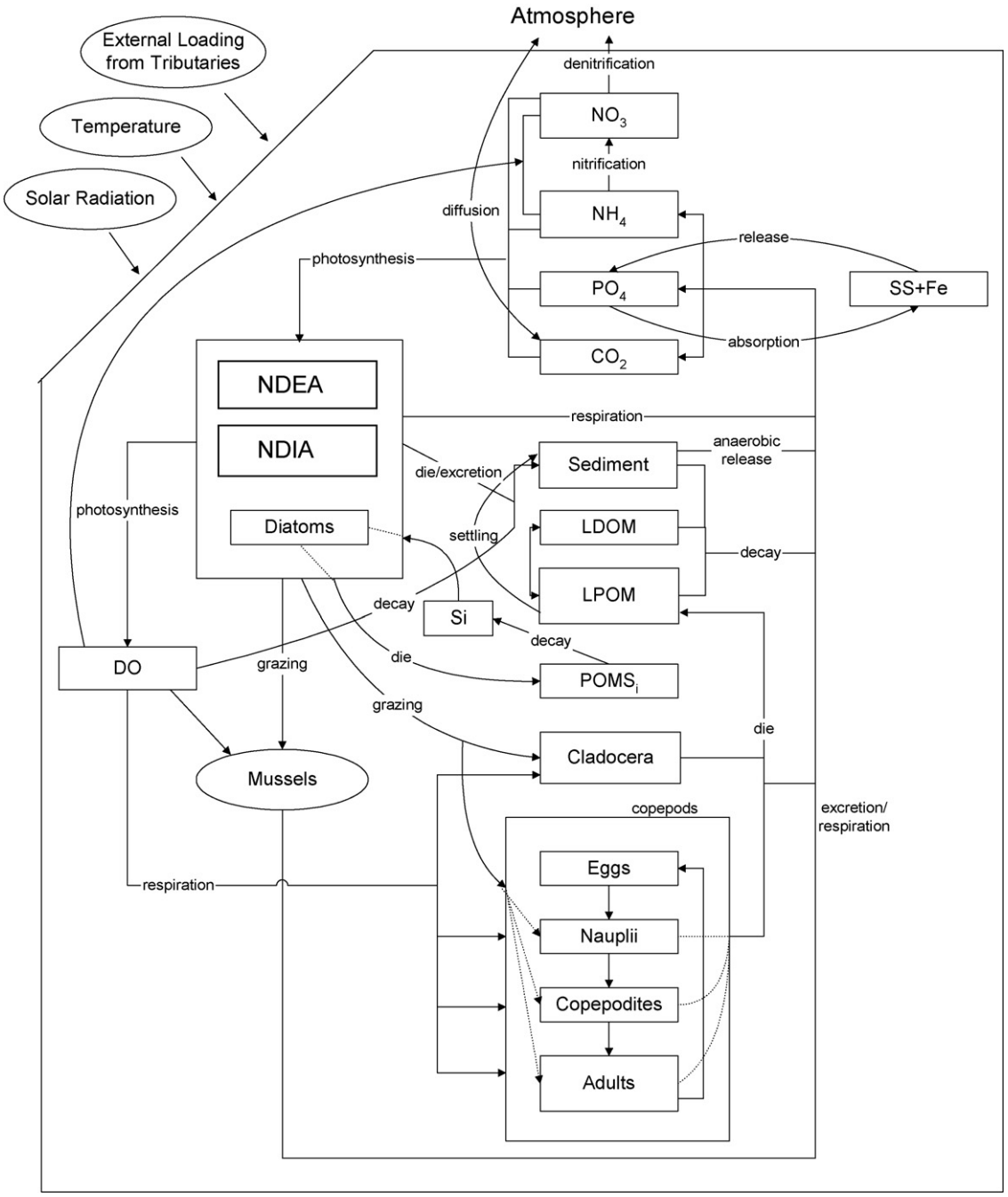

Fig. 2 – Model structure of the chemical and biological components of EcoLE.

(Hartley and Potos, 1971).

$$\lambda_T = 0, \quad \text{if } T \le T_1$$

$$\lambda_T = \frac{K_1 e^{\gamma_1 (T-T_1)}}{1 + K_1 e^{\gamma_1 (T-T_1)} - K_1} \frac{K_4 e^{\gamma_f (T_4 - T)}}{1 + K_4 e^{\gamma_f (T_4 - T)} - K_4}, \quad \text{if } T_1 < T < T_4$$

$$\lambda_T = 0, \quad \text{if } T = T_4$$

where,

$$\gamma_1 = \frac{1}{T_2 - T_1} \ln \frac{K_2(1-K_1)}{K_1(1-K_2)}$$

$$\gamma_2 = \frac{1}{T_4 - T_3} \ln \frac{K_3(1-K_4)}{K_4(1-K_3)}$$

2.2.3. *Light limitation* (λ_I)

We adopted Steele's (1962) formulation to simulate the light limitation, which includes photoinhibition effects.

$$\lambda_I = \frac{I}{I_s} e^{(1-(I/I_s))}$$

where, I_s is the saturating light intensity, I the available light intensity at depth z: $I = (1-\beta) I_0 e^{-\eta Z}$, I_0 the light intensity at

water surface, β the fraction of solar radiation absorbed at the water surface, and η is the light extinction coefficient, combination of the extinction effects of water, inorganic and organic suspended solids, and algae.

2.2.4. *Nutrient limitation (λ_i)*

Nitrogen and phosphorus are the most commonly modeled limiting nutrients, plus silicon for diatoms. The most commonly used formulation for computing the nutrient limiting factor is based on the Michaelis–Menten or Monod relationship, which assumes that the nutrient compositions of the algal cells remain constant and the external nutrient concentrations Φ of available nutrients (i) affect the algal growth rates by a factor, λ.

$$\lambda_i = \frac{\Phi_i}{P_i + \Phi_i}$$

where P_i is the half-saturation constant for the nutrient i.

Between nitrate and ammonia, algae prefer ammonia. This preference is expressed as a preference factor (P_{NH_4}) (Cole and Wells, 2003):

$$P_{NH_4} = \Phi_{NH_4} \frac{\Phi_{NO_3}}{(K_{NH_4} + \Phi_{NH_4})(K_{NH_4} + \Phi_{NO_3})} + \Phi_{NH_4} \frac{K_{NH_4}}{(\Phi_{NH_4} + \Phi_{NO_3})(K_{NH_4} + \Phi_{NO_3})}$$

We assume that zooplankton selectively graze on algae, which are modeled by assigning a weight to each algal group, i.e., 1.0 for NDEA, 0.5 for diatoms (Scavia et al., 1988) and 0 for NDIA. We further assume that mussels graze on NDEA and diatoms indiscriminately (Fanslow et al., 1995; Horgan and Mills, 1997). However, as blue-green algae are selectively rejected by dreissenid mussels (Vanderploeg et al., 2001), we set the net loss of blue-green algae due to mussel grazing to zero.

All algal and biochemical parameter values are listed in Appendix A.

2.2.5. *Zooplankton*

The energy fixed by phytoplankton moves up to zooplankton, which further affects fish recruitment. Cladocerans and copepods are the two dominant zooplankton groups in Lake Erie after May (Wu and Culver, 1991). Their grazing results in a clear-water phase in mid summer (Wu and Culver, 1991), so we focused on these two crustacean groups. We adopted Fennel and Neumann's (2003) stage-structured population model for copepods for use in our model. This copepod population submodel contains four state variables: copepod egg biomass (Z_e), copepod nauplius biomass (Z_n), copepod copepodite biomass (Z_c), and copepod adult biomass (Z_a). We used a general mass conservation model, modified from Scavia et al.'s (1988) model for Lake Michigan to simulate cladocerans (Appendix B). We assume that crustaceans consume edible algae (NDEA and edible diatoms) as well as non-living organic particles (Talling, 2003).

2.2.6. *Mussels*

Two dreissenid mussel processes are included in the EcoLE model, i.e., grazing on phytoplankton and excretion of N and P nutrients (Table 1). Predation of zooplankton by mussels is not included in the model. Although mussels have been shown to ingest rotifers in aquarium experiments (MacIsaac et al., 1991), there is no evidence of ingestion of copepod nauplii or large zooplankton (cladocerans and copepods) (MacIsaac et al., 1995). Moreover, it is unknown how much access they have to zooplankton in the field. Field observations showed that there is no significant difference of cladoceran and copepod abundance between before and after mussels' colonization (MacIsaac et al., 1995; Noonburg et al., 2003).

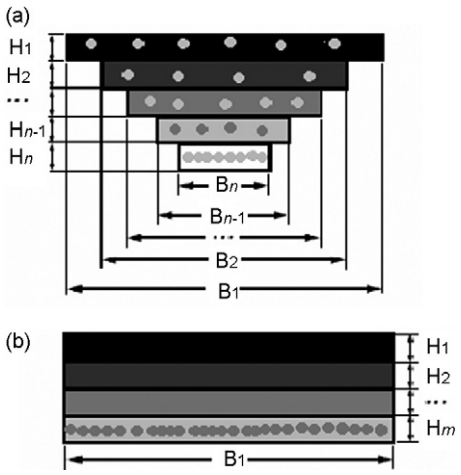

Fig. 3 – Reshaping the western basin from staircase (a) to rectangular box (b) by keeping surface area B_1 constant and adjusted depth H_i so that $B_1\sum_{i=1}^{m}H_i \approx \sum_{i=1}^{n}B_iH_i$, where $m \le n$. The adjustment allows estimation of the effects of dreissenids, which are distributed only in the bottom cell of the rectangular box. The gray dots indicate the location of dreissenid mussels, while dreissenid population in a model cell is determined by the sedimental area and mussel density.

EcoLE is a two-dimensional model, with individual cells 1-m thick, ~2 km long and as much as 80 km wide. It averages conditions along each cell's width so mussels in the nearshore and the offshore have equal access to the algae found in that same model cell. This introduces a systematic error because mussels are only located in the nearshore zone (and to a lesser extent offshore) in contact with the sediment. They have a much smaller contact area with the contents of the cell, which is much less than the cell's whole bottom area. To minimize this error, we adopted Boegman et al.'s (2008b) approach to reshape each modeling segment (water column) in the shallow and flat western basin from a step staircase-shaped box to a rectangular box. Briefly, we held the surface area of each 2-km long segment constant and adjusted the depth (1 m resolution) until the volume of the rectangular box (segment) is close to the real volume of the segment measured from the bathymetry. After the adjustment, all cells in a given segment have the same dimensions (km × km × m). Mussels are now located only in the bottom cell, which has a sediment area equal to the surface area of the segment (Fig. 3b). The deeper central and eastern basins are not reshaped and mussels are located in each cell (Fig. 3a), and thus the effects of dreissenids

Table 1 – Kinetic rates of dreissenid mussels used in the EcoLE model

	Western basin	Central basin	Eastern basin
Length (mm)–mass (mg) regression	$DW = 0.0057L^{2.732}$ [a]	$DW = 0.0046L^{2.848}$ [a]	$DW = 0.004L^{2.96}$ [b]
Clearance rates ($l\,h^{-1}$)	$FR = 1.919DW(g)^{0.88}$ [c]	$CR = 0.2221DW^{0.5419}$ [d]	$CR = 0.2221DW^{0.5419}$
Clearance rates ($m^3\,d^{-1}$)	$FR = 0.046DW(g)^{0.88}$	$CR = 0.005DW^{0.5419}$	$CR = 0.005DW^{0.5419}$
N excretion rate ($\mu g\,N\,mg\,DW^{-1}\,d^{-1}$)	$\log_{10}(NH_4) = 0.379\log_{10}(DW) + 0.021$ [a]	$\log_{10}(NH_4) = 0.379\log_{10}(DW) + 0.021$ [a]	$\log_{10}(NH_4) = 0.379\log_{10}(DW) + 0.021$ [a]
P excretion rate ($\mu g\,P\,mg\,DW^{-1}\,d^{-1}$)	$\log_{10}(PO_4) = 0.505\log_{10}(DW) - 1.172$ [a]	$\log_{10}(PO_4) = 0.297\log_{10}(DW) - 1.195$ [a]	$\log_{10}(PO_4) = 0.297\log_{10}(DW) - 1.195$ [a]
O_2 consumption rates ($mg\,O_2\,g\,DW^{-1}\,d^{-1}$)	1.0 [f]	6.0 [f]	6.0 [f]

[e] Arnott and Vanni (1996).
[a] Conroy et al. (2005a).
[b] Roe and MacIsaac (1997).
[c] Pontius (2000) (we assume particle removal is 100%).
[d] Baldwin et al. (2002).
[f] This study.

are averaged through the full volume of the cell with which they have contact.

Zebra mussels have been more or less replaced by quagga mussels recently (Stoeckmann, 2003), such that by 1998, 84.4% of mussels in the eastern basin and 99.7% in the central basin were quagga mussels, but only 36.9% in the western basin (Jarvis et al., 2000). We assume therefore, for simplicity, that during the 1997–1999 period mussels in the western basin were 100% zebra mussels, whereas those in the central and the eastern basins were 100% quagga mussels. As their density distribution and size frequency vary greatly in time and space, there has never been a good estimation of the two populations. Nevertheless, we used the depth-dependent estimations by Jarvis et al. (2000) in EcoLE (Table 2). Thus, dreissenid population size in each model cell is the product of depth-dependent density ($ind\,m^{-2}$) and the sediment area (m^2) of each model cell. As a first approximation, we assumed that these mussels are uniform in size (10 mm in length). Using size-frequency and depth-dependent density data from Jarvis et al.'s Figs. 7–20 (see Table 2) and length-mass equations (Table 1), we calculated Jarvis et al.'s mussel population soft-tissue biomass ($g\,DW\,m^{-2}$), and found that their population biomass estimate is very close to that for our 10-mm simulated mussel population (Table 2).

We then varied mussel densities and lengths during our sensitivity analysis to assess the effects of variation in mussel population densities and size distribution on our simulation of dreissenid impacts on the phytoplankton and nutrients.

2.2.7. *Nutrients*

We modified Cole and Buchak's (1995) nutrient submodels to include recycling components by crustaceans and dreissenids, through respiration, excretion, ingestion, and egestion in the corresponding nutrient pools or pathways (Zhang, 2006).

Instead of using a constant sediment oxygen demand (SOD), we expressed SOD as a function of oxygen concentration and temperature (Lucas and Thomas, 1972; Lam et al., 1987).

$$S_{od} = S_{od_{max}} \frac{\Phi_{DO}}{\Phi_{DO} + O_h} \theta^{(T-20)}$$

$S_{od_{max}}$, maximum sediment oxygen demand at 20 °C, $g\,O_2\,m^{-2}\,d^{-1}$; O_h, oxygen concentration half-saturation constant, $1.4\,g\,O_2\,m^{-3}$.

2.3. *Initialization, calibration, and validation data sources*

It is challenging to collect all the data needed to initialize and calibrate such a complex ecosystem model. We appreciate the extensive help we received from many agencies and individuals (Table 3). This model incorporates inflows from eight tributaries of Lake Erie, including rivers and wastewater treatment plants (WWTPs), namely the Detroit, Maumee, Sandusky, and Cuyahoga Rivers and Ohio's Toledo, Cleveland Westerly, and Cleveland Easterly WWTPs, and Pennsylvania's Erie WWTP. For each tributary, flows, nutrient concentrations, and water temperatures are needed. Outflows are needed for two withdrawals, the Niagara River and the Welland Canal. Climate data include wind speed, wind

Table 2 – Comparisons of mussel biomass (g DW m^{-2}) between Jarvis et al.'s population with various sizes and EcoLE's 10-mm mussel population

Depth (m)	Density (ind m^{-2})	Biomass (g DW m^{-2})					
		WB		CB		EB	
		Jarvis et al.'s	10 mm	Jarvis et al.'s	10 mm	Jarvis et al.'s	10 mm
0–5	2927	10.8	9.0	14.8–62.8	9.5	9.9–36.5	10.7
5–10	6419	23.8	19.7	32.4–137.7	20.8	21.7–80.0	23.4
10–20	3233	12.0	9.9	16.3–69.4	10.5	11.0–40.3	11.8
20–30	3431			17.3–73.6	11.1	11.6–42.8	12.5
30+	3172			16.0–68.0	10.3	10.7–39.5	11.6

direction, cloud cover, precipitation, dew point and air temperatures.

Monthly or semimonthly physical, chemical and biological data needed to initialize the water quality state variables, and calibrate and verify the model were taken from the Ohio State University's LEPAS database. The sampling sites of 1997, 1998 and 1999 are consistent among years (Fig. 1).

2.4. *Error analysis*

Paired *t*-test (MINITAB 14) is used to test for significant differences ($p < 0.05$) between the means of predictions and field measurements.

Mean relative error (Lam et al., 1983) is also used to assess the adequacy of the model, which is defined as $E = 1/N \sum |\hat{c}_i - c_i|/\hat{c}_i$, where $\hat{c}_i$ and c_i are the observed and the modeled values, respectively, and N is the number of pairs of the observed and modeled values. The median relative error refers to the mean relative error of the first 50% of the relative error samples which have been arranged in order of increasing difference between the observed (field) data and those simulated by the model. The median relative error is regarded as a useful error statistic (Di Toro, 1983; Lam et al., 1983).

3. Simulation and results

3.1. *Physical simulation*

The temperature in the western basin was relatively homogeneous with depth most of the time. Weak stratifications in the western basin were partially due to the biased tempera-

Table 3 – Input data needed to run EcoLE and their sources

Location	Data	Data sources
Cleveland Easterly WWTP	Constituent concentrations*, inflow and water temperature	Sandra Kemper, OHEPA
Cleveland Westerly WWTP	Constituent concentrations, inflow and water temperature	Sandra Kemper, OHEPA
Erie WWTP	Constituent concentrations, inflow and water temperature	Nichole Maywah, OHEPA
Toledo WWTP	Constituent concentrations, inflow and water temperature	Sandra Kemper, OHEPA
Maumee River	Constituent concentrations, inflow and water temperature	Peter Richards at Heidelberg College and Mary Ann Silagy, OHEPA
Sandusky River	Constituent concentrations, inflow and water temperature	Peter Richards, Heidelberg College and Mary Ann Silagy, OHEPA, Douglas A. Keller, OHEPA, Division Of Drinking and Ground Waters
Detroit River	Constituent concentrations, inflow and water temperature	Richard N. Lundgren, DEQ Surface Water Quality Division, Lansing, MI; John Koschik, Hydraulic Engineer, USACE, Detroit District, Great Lakes Hydraulics and Hydrology Office
Cuyahoga River	Constituent concentrations, inflow and water temperature	Peter Richards at Heidelberg College, and USGS (http://waterdata.usgs.gov/nwis/)
Niagara river at Buffalo, NY	Flows	Tim Hunter, NOAA/GLERL (Great Lakes Environmental Research Laboratory)
Welland Canal	Withdrawals	Tim Hunter, NOAA/GLERL
Lake Erie	Bathymetry file	Boegman et al. (2001)
Over Lake Erie	Precipitation	Tim Hunter, NOAA/GLERL
Over Lake Erie	Meteorological data	http://www.ncdc.noaa.gov/pdfs/lcd/lcd.html
Lake Erie	Initialization of state variables	LEPAS database in OSU

*Constituents include suspended solid, labile dissolved organic mater, soluble reactive phosphorus, ammonium, nitrate + nitrite, dissolved oxygen, biochemical oxygen demand, silicon. Available constituents of each tributary varied.

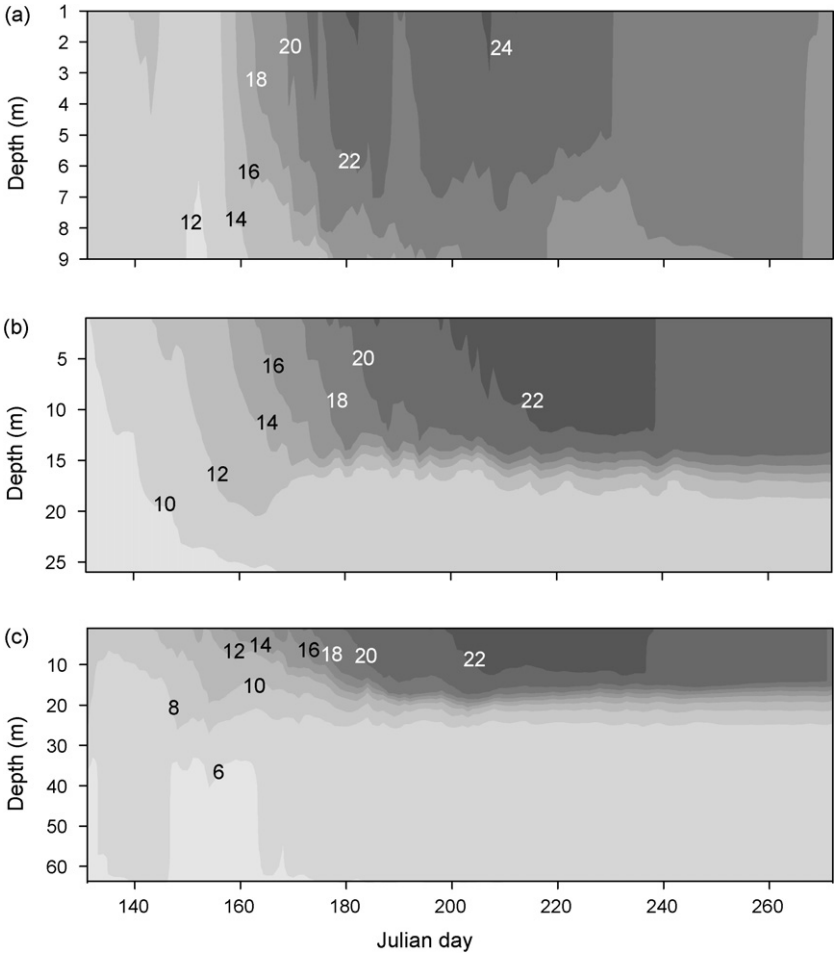

Fig. 4 – The 1997 simulation of vertical distributions of temperature outputs of EcoLE from representative segments in the western basin (segment 30, 9 m, (a)), central basin (segment 95, 26 m, (b)) and eastern basin (segment 175, 64 m, (c)) over the simulation period. Simulated dates were 10 May to 30 September. Note the different scales on the y-axis.

ture sampling from the model, which occurred at noon each day, so the model results reflect diel thermal stratification. In the central and eastern basins, however, the model showed a strong seasonal thermal stratification with durations of over 2 months (e.g., in 1997, Fig. 4).

We used surface and bottom water temperature measurements taken with the plankton collections to evaluate the success of the physical simulation. Comparisons of the monthly means from the simulations and field measurements show that simulated temperatures agree with field measurements well for all three basins, e.g., 1997 (Fig. 5). The differences between simulated and measured monthly means are all less than 1.2 °C for bottom temperatures. The differences are higher for the surface temperatures. Most of them are less than 2.0 °C, except those of the eastern basin in June. For 1998 and 1999, there is good agreement between modeled surface and bottom temperatures and field-measured values. From this, we conclude that using Cole and Buchak's (1995) algorithm and cloud cover data from National Oceanic and Atmospheric Administration (NOAA) adequately reflects the radiant input to the lake, and that the absence of irradiance data from on-lake buoys is not a major problem.

3.2. *Chemical–biological simulations*

We used 1997 for the calibration year for six state variables: NDEA, diatoms, copepods, cladocerans, total dissolved phosphorus (TP-F), and ammonia (NH_4) (Fig. 6), while 1998 and 1999 are verification years. During verification, all parameters calibrated in 1997 were kept intact for 1998 and 1999, while the meteorological data, external loading, and initial values of state variables of the verification years are used in the simulations. In 1997, the model simulations match the field observations well for diatoms, TP-F, and NH_4. However, the model predicts lower values of NDEA, copepods and cladocerans in the west-central basin (segments 50–80, near the mouth of the Sandusky River) than we found in field measurements. Similar simulation results occur in verification years, 1998 and 1999 (Figs. 7 and 8), except that simulated biomass of copepods matched the high values found in the samples collected in the west-central basin. Even when the maximum growth rate of NDEA is increased, the model-predicted values are still lower than the field observations. Calibrating the model with these unnaturally high maximum growth rates would deplete the nutrients and slow algal growth. In the west-central basin, the high observed values of NDEA are likely due to inputs

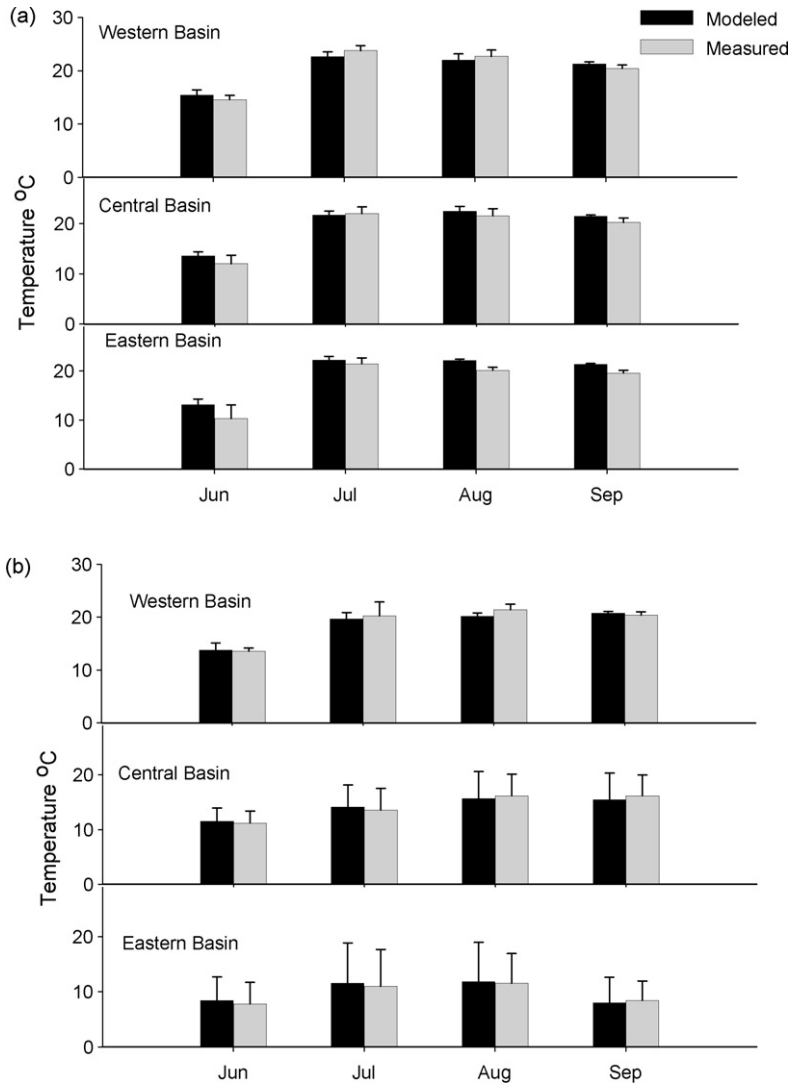

Fig. 5 – 1997's comparisons between the modeled and the observed surface temperatures (a) and bottom temperatures (b). The light bars are means of temperatures measured in the month and the basin. The dark bars are means of temperatures sampled in the model output corresponding to dates and locations (segments) of the field measurements. Error bar represents one standard deviation of the mean.

from other sources, such as loading from tributaries, or resuspension of algae from the bottom. The low predicted values of cladoceran biomass in the west-central basin are a consequence of the low predicted values of NDEA. Compared with the good match between simulations and observations of copepods in 1998 and 1999, the lower prediction in 1997 may indicate that the start date of simulation is also important. Simulation in 1997 started on 10 May, which is 10 days earlier than 1999 and 20 days earlier than 1998. The recruitment from diapausing eggs might still play an important role in copepod population dynamics during this time in 1997, however, this process is not considered in the model.

The simulations of NDIA are not calibrated and verified because of a paucity of initial data. In late May or early June there are few *Microcystis* colonies observed in the water column, which means most of the model cells have no NDIA at the beginning of the simulations. Cyanobacterial populations in the lake begin from resting cells in the surficial sediments and/or from riverine inputs. Nevertheless, simulation of NDIA dynamics was also investigated by adding an arbitrarily small amount of NDIA as "seeds" on the lake bottom to replace the zeros collected from the field. To examine the agreement of the model's estimate of NDIA relative to field measurements, we averaged NDIA biomass for August and September for both field measurements and corresponding model predictions for all 3 years (Fig. 9). We chose August and September because during these two months blue-green algal blooms are obvious (if they occur). The model's predictions of NDIA biomass are similar to field measurements for 1997 and 1999. Our model does predict higher abundance of NDIA in the western basin for 1998, but these results are still 90% lower than the field measurements. As the many NDIA loading sources are not considered in the model, it is not surprising that our model does not predict

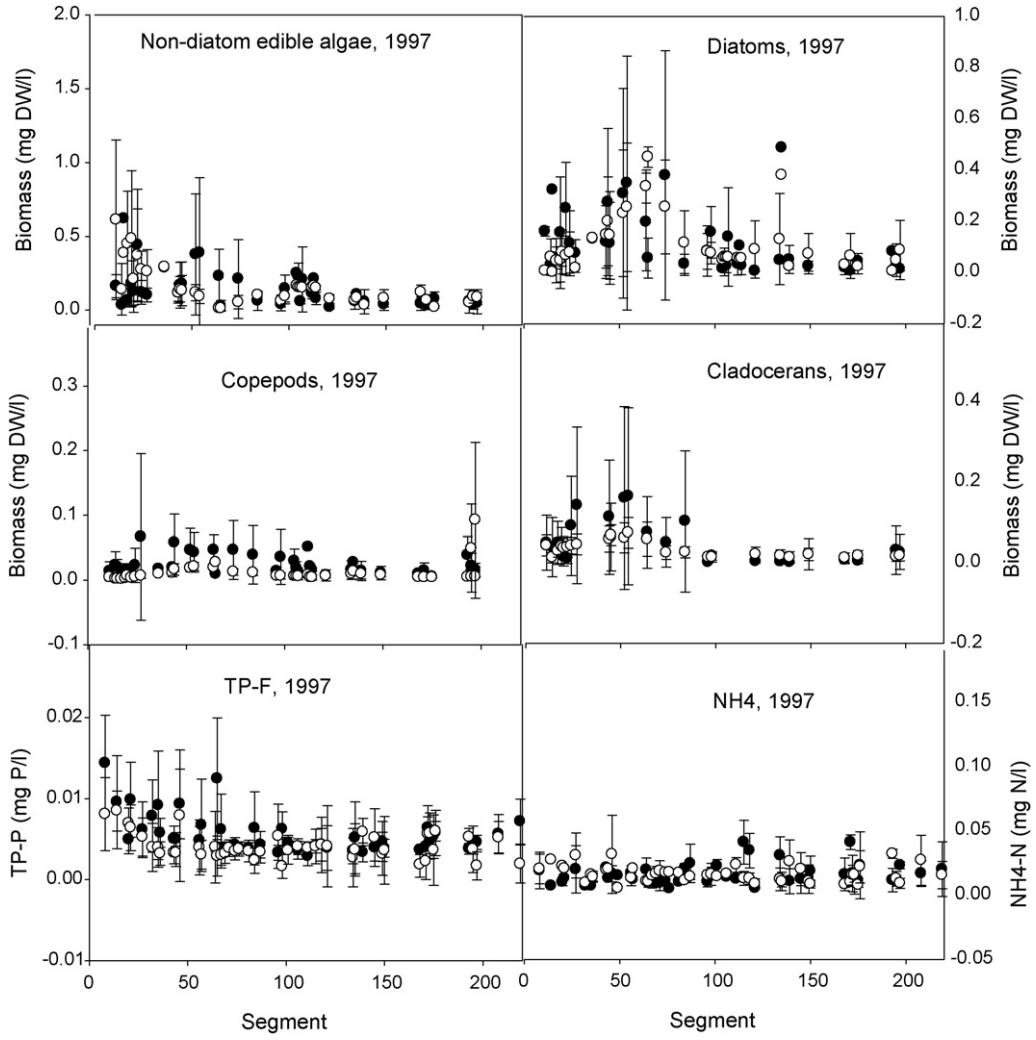

Fig. 6 – Model calibration (year 1997) for non-diatom edible algae, diatoms, copepods, cladocerans, TP-F, and NH_4. Plotted values represent seasonal averages for field observations (solid circles) and model predictions (open circles) of field sampling segments from west (1) to east (220). The western basin ends at segment 49, and the central basin ends at segment 156.

the high NDIA abundance in the western basin observed in 1998.

3.3. *Error analysis*

Paired *t*-tests (Table 4) show that the modeled values and field measurements do not differ for most cases. The few cases that are significantly different are not surprising, given the complexity of the ecosystem and the processes missing from the model (e.g., nearshore–offshore gradients, algal loading from rivers, P loading from unmonitored non-point sources, etc.). Because we use this model to investigate the impacts of the external phosphorus loading program on the Lake Erie ecosystem, we worked to be sure that the phosphorus simulation is realistic. Although the differences between the model's monthly means and the field observations' are significant for four cases, those differences are very small and below the field measurement precision ($0.01\,mg\,l^{-1}$).

Median relative errors (Fig. 10) are all below 50% for all six state variables in all three years. For 1997, TP-F has the lowest median relative error, 12%, while Copepods has the highest, 47%. For 1998, NDEA has the lowest, 17%, while Diatoms has the highest, 32%. For 1999, NH4 has the lowest, 16%, while Diatoms has the highest, 41%. In general NDEA, TP-F and NH4 have lower median relative errors and Diatoms and Copepods have higher median relative errors. The median relative errors of TP-F are below 20% for all 3 years.

3.4. *Dreissenid impacts on phytoplankton and nutrients*

The filtering rate is the volume of water that an individual organism filters per day ($ml\,ind^{-1}\,d^{-1}$) and clearance rate is the volume of water that an individual organism clears per day ($ml\,ind^{-1}\,d^{-1}$) (Wu and Culver, 1991). Only if the organism can clear all food particles in the water as it filters (100% removal) and avoids refiltering water it has already processed are the clearance rates equal to the filtering rates. In dreissenids, these rates are a function of body mass (Table 1). The grazing rate of a population ($mg\,m^{-2}\,d^{-1}$) is a product of

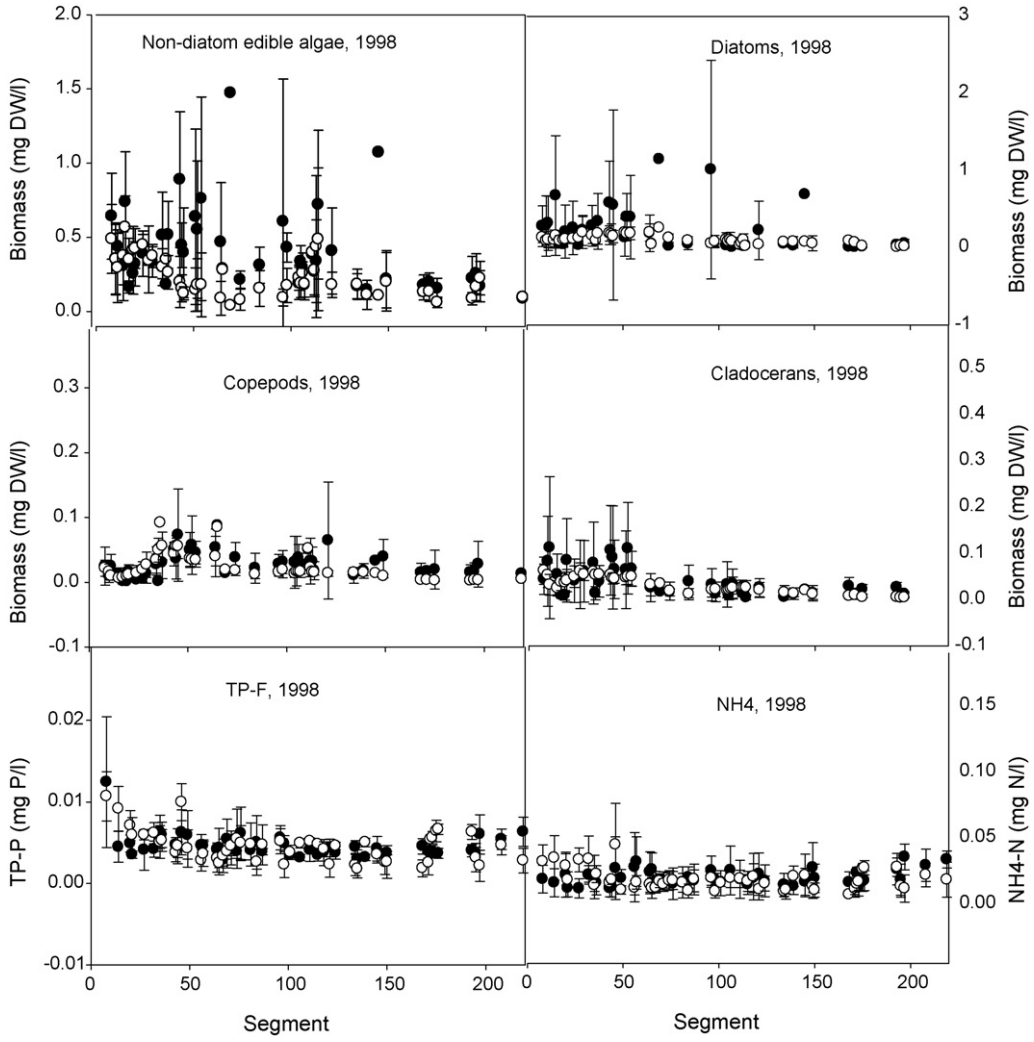

Fig. 7 – Model verification of 1998 for non-diatom edible algae, diatoms, copepods, cladocerans, TP-F and NH_4.

the clearance rate and the food particle concentration in the water ($mg\,l^{-1}$) and the number of individuals in the population ($ind\,m^{-2}$).

We estimate the dreissenids' grazing impacts, defined as the percentage of algal biomass of the whole basin or lake that is grazed by dreissenid populations in a given period of time. Thus, the daily grazing impacts of dreissenids (I) on algae are computed as the percentage of algal biomass (B) that is grazed by dreissenids (G) during one day in the basins. The grazing rates (g_j) of mussels in model cell j are the product of mussel clearance rates (c_j) and the algal concentration (b_j) and the number (n_j) of mussels in the model cell. That is, we assume only algae in the same model cell with dreissenids are instantaneously available to the mussels. Algae in other model cells will be available to dreissenids only when they are transported or sink into the model cell where dreissenids are located.

$$G = \sum_j g_j, \quad \text{where } g_j = c_j b_j n_j$$

$$I(\%) = \frac{G \times 100}{B}$$

Model results suggest that in the western basin dreissenids clear 20% of the water daily, while the grazing impacts on NDEA are only 6, 4, and 10% for 1997, 1998, and 1999, respectively, and on diatoms the impacts are 7–8% for all three years (Table 5). In the central and the eastern basins, dreissenids clear 3% of the water daily, while the grazing impacts on NDEA and diatoms are around 1% in the central basin and 1–2% in the eastern basin. NDIA are selectively rejected by dreissenids and zooplankton. Therefore, there is no direct grazing impact by dreissenids on NDIA.

Nutrient excretion per day by dreissenids in each model cell is estimated as the product of lab-measured individual nutrient remineralization rates of phosphorus or nitrogen (Table 1) and the number of mussels of the model cell. They excrete each day an amount of SRP equivalent to a high proportion of the water column SRP in the western basin: 23% in 1997, 19% in 1998 and 56% in 1999, whereas the proportions decrease to about 1% in the central and the eastern basins (Table 6) due to the large water volume of the basins and the lower mass-specific phosphorus excretion rates of quagga mussels.

Dreissenid mussels' mean daily NH_4-N excreta contribute 13% of the total nitrogen (NO_3-N and NH_4-N) in the water col-

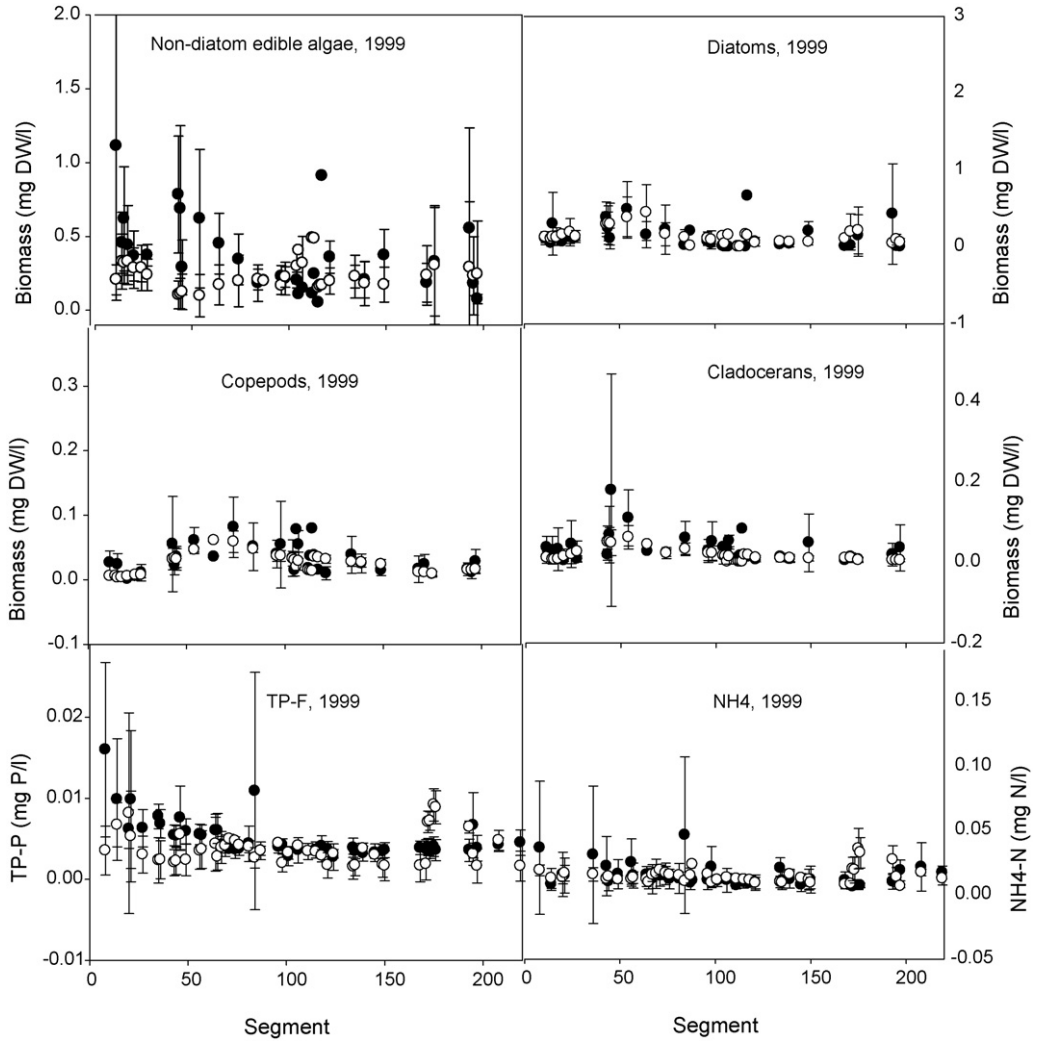

Fig. 8 – Model verification of 1999 for non-diatom edible algae, diatoms, copepods, cladocerans, TP-F and NH_4.

umn in 1997, 12% in 1998 and 15% in 1999 in the western basin (Table 6), and 4% in the central basin.

3.5. *Model sensitivity analysis: dreissenid population estimates*

Because no direct measurements of dreissenid population structure (density and size frequency) were available for any year, densities and shell lengths of mussels were varied under the model conditions of year 1997 to investigate the sensitivity of the model to mussel density and mussel size. Specifically, we repeated simulations with dreissenid densities at 0.1, 1.0, 10, and 20 times of density estimates from Table 3.2, and repeated the simulations for mussels at four sizes (body length = 5, 10, 15, and 20 mm) for each population density option.

3.5.1. *Impacts on NDEA*

Model results show that an increasingly small mussel population (combination of low density and small body size) will decrease NDEA biomass, but increasingly large mussel populations will increase NDEA biomass (Fig. 11a). These results suggest that when mussels first invaded Lake Erie and their population density was small, decreases in algal biomass and increases in water clarity would be expected. However, when the mussel population grew larger, a further depletion of edible algae in the water column should not be expected. Instead, we predict more NDEA algae in the water column due to nutrient excretion.

In the western basin, a small dreissenid population (5-mm body length) tends to increase its grazing impact with increases in its population size, while a large mussel (15 or 20 mm) population tends to decrease its grazing impact with increases in its population size (Fig. 11b). Interestingly, the larger mussel population sizes (high densities and large body size), that result in the highest NDEA biomass and production in the water column, have smaller population grazing impacts. This indicates a strong algal concentration boundary layer above the mussel bed, and the ability of excreted nutrients to diffuse into the euphotic zone.

In the central and eastern basins, grazing impacts increase consistently and dramatically with increasing mussel population density or mussel body size or both, likely because mussels are located in each model cell throughout the water

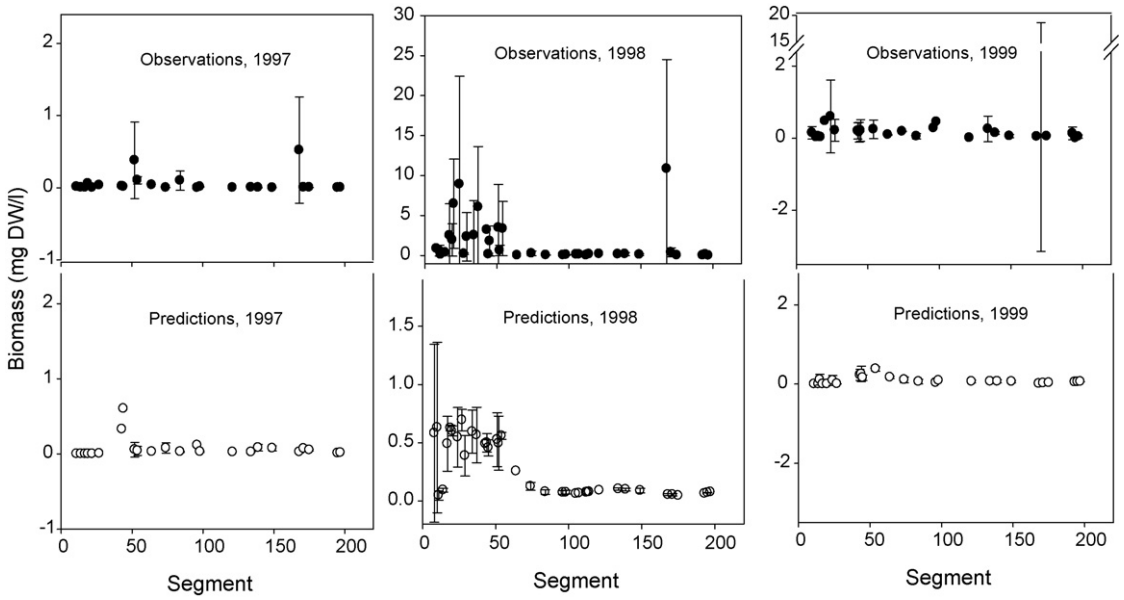

Fig. 9 – Comparisons of NDIA biomass between observations and predictions for 1997, 1998, and 1999. NDIA biomass are averages of August and September. Note the different scales on the y-axis of 1998.

column in these two basins. The lack of a third dimension in the model allows mussels situated on the south shore to consume algae at both the south and north shores, which is not true in the field. Thus, the mussel grazing estimates from the EcoLE model for the central and the eastern basins are more like estimations from a previous study, Edwards et al.'s (2005) fully mixing model, while the case in the western basin is more realistic.

Table 4 – Results of paired *t*-test ($p < 0.05$) of the mean difference between modeled and observed values of six state variables for 3 years

	WB	CB	EB
1997			
NDEA	+	+	+
Diatoms	+	+	+
Cladocerans	+	+	+
Copepods	–	–	+
TP-F	–	–	+
NH_4	–	+	+
1998			
NDEA	+	–	+
Diatoms	–	+	+
Cladocerans	+	+	–
Copepods	+	–	–
TP-F	+	+	+
NH_4	–	–	+
1999			
NDEA	–	+	+
Diatoms	+	+	+
Cladocerans	+	–	+
Copepods	+	+	+
TP-F	–	–	+
NH_4	+	+	+

"–" indicates significant difference; "+" indicates no significant difference.

3.5.2. *Impacts on diatoms*

Model results show that mussel impacts on diatoms are more complicated than those on NDEA in the western basin. On NDEA biomass, the impacts have only one turning point as mussel population increases, whereas diatom biomass first decreases, then increases, then decreases as dreissenid biomass increases (Fig. 11a). In the central and eastern basin, mussels decrease diatom biomass consistently with increasing density or mussel size. However, the boundary layer shows less effect on dreissenid grazing for diatoms than for NDEA, probably due to the higher sinking rates of diatoms (Fig. 11b).

3.5.3. *Impacts on non-edible algae (NDIA)*

Mussels increase NDIA biomass consistently with increasing density or body size for all three basins (Fig. 11a). High biomass occurs with large mussel populations. Noticeably, with the largest mussel population (20-mm and 20-fold) NDIA productivity exceeds NDEA productivity in the western and eastern basins.

3.5.4. *Effects on nutrients*

With increases in mussel density and body size, the mussel population PO_4^{3-} and NH_4^+ excretion rates increase consistently and rapidly (Fig. 12), because the excretion rates are an exponential function of individual body mass, which is in turn an exponential function of body length (or "size" as used here).

4. Discussion

4.1. *Physical simulations*

The simulated seasonal temperature distributions show that there is no strong seasonal thermal stratification in the west-

Table 5 – Basin-wide impacts of dreissenids on NDEA (non-diatom edible algae) and diatoms

	Unit	1997			1998			1999		
		WB	CB	EB	WB	CB	EB	WB	CB	EB
Basin water volume	km^3	24	316	161	24	316	161	23	309	159
Water processed by mussels	$km^3\ d^{-1}$	5	10	5	5	10	5	5	10	5
	%	21	3	3	21	3	3	22	3	3
Basin-wide NDEA	mt DW	6712	26,320	7982	6903	43,849	17,561	4595	47,862	28,119
NDEA grazed by mussels	mt DW d^{-1}	414	173	99	282	346	245	443	445	465
	%	6	1	1	4	1	1	10	1	2
Basin-wide diatoms	mt DW	1625	27,429	4576	4766	32,416	5,522	4175	31,162	14,006
Diatom grazed by mussels	mt DW d^{-1}	108	294	60	345	405	73	344	367	219
	%	7	1	1	7	1	1	8	1	2

ern basin. However, it is not always thermally homogeneous either. The weak diel stratification simulated by EcoLE has been observed by several field studies and thought to be crucial for understanding the impact of dreissenid mussels on Lake Erie (Ackerman et al., 2001; Edwards et al., 2005; Boegman et al., 2008a) and mayfly (*Hexagenia*) nymph survival (Bridgeman et al., 2006; Loewen et al., 2007). The duration of simulated seasonal stratifications in the central basin and the eastern basin (Fig. 4) agree well with that reported by Schertzer et al. (1987). The water starts to stratify in early June and becomes firmly stratified in early July. Fall turnover begins by the end of September and stratification disappears by the end of October (Fig. 4). Results of this study also show that there are relatively homogeneous temperatures within the epilimnion and hypolimnion, while the metalimnion becomes thinner with time. McCune (1998) and Edwards (2002) studied the mixing processes in the central basin and found a pattern similar to the results of this study. Modeled temperatures of the surface and bottom water of Lake Erie show good agreement with the field observations. Moreover, model performance is not limited to the thermal structure. The dominant longitudinal currents associated with storm surges and surface seiches are also well simulated (Boegman et al., 2001). With these results, we consider that EcoLE catches the major characteristics of the physical processes that can affect the chemical and biological processes in the lake.

4.2. *Chemical and biological simulations*

The EcoLE model chemical and biological simulations show good agreement with field observations. However, we also see large standard deviations among the field observations as well as in the simulations. EcoLE is a complex model with numerous parameters and equations. The intensive monitoring program (sampled monthly, with some stations of some years sampled weekly) provides hundreds of observational data for calibration and verification. However, these data are still sparse for a model with high temporal and spatial resolution. For example, spatial interpolation has to be used to initialize the state variables for most of the segments, which may misrepresent the patchiness of phytoplankton and zooplankton. Another source of error could be the inherent limitation of a laterally averaged two-dimensional model. The model cannot simulate the differences between nearshore and offshore observations. However, we could not arbitrarily discard either the nearshore or offshore field data, lest we make the already sparse field data become even less abundant. Furthermore, plankton abundance is not always significantly different between nearshore and offshore sites (Wu and Culver, 1994). Thus, data of each segment were averaged and investigated together with their standard deviations. Uncertainties also arise due to the simplified dreissenid population distribution used in the model. It is quite possible that the population densities are, in fact, ten times higher or lower than the ones we used in the model. Our uncertainty analysis shows that 10-fold differences in the dreissenid population density result in significant differences in the lake-wide means of a mass of state variables (Table 7). Despite the above conditions, our model still holds the main characteristics of bio-chemical processes in Lake Erie. Thus, we are confident in use of this model to analyze ecological processes qualitatively, if not quantitatively.

Table 6 – The relative importance of nutrients excreted by dreissenid mussels to the basin-wide nutrient mass

	Unit	1997			1998			1999		
		WB	CB	EB	WB	CB	EB	WB	CB	EB
Basin-wide SRP-P	mt P	28.6	837.0	515.4	34.2	1203.4	824.8	11.9	809.6	825.1
P excretion by dreissenids	mt P d^{-1}	6.6	13.6	6.4	6.6	13.6	6.4	6.6	13.6	6.4
	%	23.2	1.6	1.2	19.4	1.1	0.8	55.5	1.7	0.8
Basin-wide NH_4-N	mt N	715.9	6357.8	4218.1	760.7	6625.3	3450.8	613.0	5729.3	4614.1
N excretion by dreissenids	mt N d^{-1}	89.6	244.0	116.7	89.6	244.0	116.7	89.6	244.0	116.7
	%	12.5	3.8	2.8	11.8	3.7	3.4	14.6	4.3	2.5

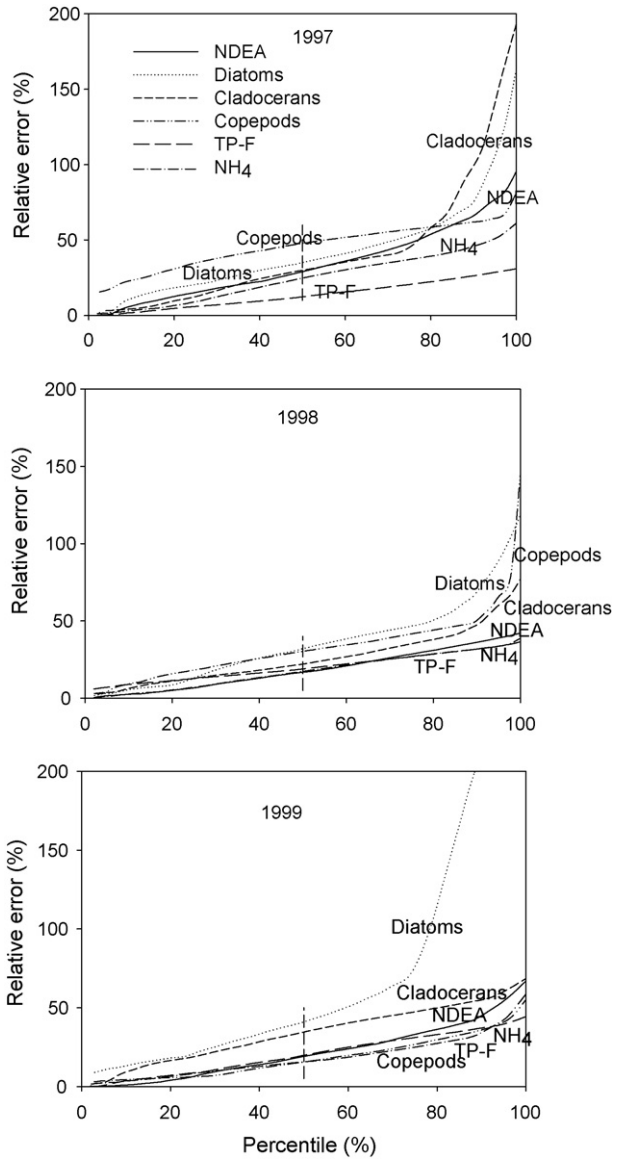

Fig. 10 – Relative error vs. sample percentile for NDEA, Diatoms, Cladocerans, Copepods, TP-F and NH_4 of 3 years. The vertical dash line indicates the median relative errors of state variables.

4.3. *Dreissenid impacts on phytoplankton*

This study showed that the grazing impacts of dreissenids are much less striking than their impacts on nutrient remineralization. At small population sizes, mussels graze NDEA down more than they stimulate the growth of NDEA by nutrient excretion. However, at higher population sizes, mussels' stimulation of NDEA growth by nutrient excretion increases dramatically, and the loss of NDEA due to grazing becomes less noticeable. Mussels increase NDIA biomass by selective rejection and, more importantly, by nutrient excretion which is more accessible to NDIA than to other algal groups.

However, previous studies emphasized the grazing impacts of dreissenid mussels. For example, MacIsaac et al. (1992) estimated zebra mussel filtering rates by combining lab-measured clearance rates with field population densities at Hen Island Reef in the western basin. Their extremely high filtering rate estimate, 132 $m^3\,m^{-2}\,d^{-1}$, brought zebra mussels to the attention of many ecologists and the public. Other early studies also showed a high grazing impact on phytoplankton in Lake Erie (e.g., Bunt et al., 1993). The observations that nearshore water became clearer (Holland, 1993; Leach, 1993) and phytoplankton biomass decreased (MacIsaac et al., 1992; Holland, 1993; Leach, 1993) in water bodies with invasion of zebra mussels supported these estimates.

Accurate estimates of the dreissenid field population density and spatial distribution is critical in estimating their grazing impacts. Our mussel densities, 2 927 or 6 419 ind m^{-2} (depth-dependent) in the western basin, are 40–90 times lower than the 2.6×10^5 ind m^{-2} estimate from Hen Island Reef that MacIsaac et al. (1992) used. Moreover, using the different size-specific filtering rates from Kryger and Riisgard (1988), Krondratev (1963), and Micheev (1966), MacIsaac et al., yield three disparate filtering rates, 132, 115, and 25 $m^3\,m^{-2}\,d^{-1}$. If the population density is changed to those we use in the model, then their filtering rates would be 1.5–3.3, 1.3–2.9, and 0.3–0.6 $m^3\,m^{-2}\,d^{-1}$, respectively. For a water column of 7 m, the updated population would process a volume equivalent to 4–47% of the water column per day. Our result of 20% per day (Table 5) is well within this range. The filtering capability of mussel populations is now far less striking than that predicted during the years when they first successfully colonized western Lake Erie. Moreover, Jarvis et al.'s (2000) basin-wide estimate of 418 ind m^{-2} is much lower than the ones we used in our simulations. Jarvis et al.'s abundance data imply even lower grazing impacts (Barbiero and Tuchman, 2004).

Besides water filtering capacity, grazing impacts of dreissenids are also affected by algal availability, which are mainly controlled by vertical mixing processes (MacIsaac et al., 1999; Ackerman et al., 2001; Noonburg et al., 2003; Edwards et al., 2005) and algal sinking rates. We found that mussels consumed few algae basin-wide from June to September. Even in the western basin, where there was no seasonal stratification and mussels had the highest impact among the three basins, the mean daily grazing impacts were only <10% of the NDEA and diatoms, which indicates that dreissenids were processing water over 50% of which had already been cleared of algae. Boegman et al. (2008a) has investigated thoroughly the vertical mixing and the formation of the boundary layer over mussel bed in the western basin. Boegman et al. (2008b) reported a daily grazing impact of ~25–30% in 1994, a little more than our results. However, their modeled algal biomass with mussels in the system is 23% lower than observations, while 8% higher than the observations when they removed mussels from the system (their Fig. 6a). They might overestimate the grazing impact because they model phytoplankton as one single algal group. For example, different algal groups have different sinking rates. Diatoms have higher sinking rates, NDEA have lower sinking rates, while some cyanobacterial algal can adjust their location in the water column and benefit more from nutrient excreted by mussels while avoiding being eaten (see discussion about NDIA). Furthermore, we calculated the daily grazing impacts of mussels and averaged them over simulation periods, while Boegman et al., compared the difference of the

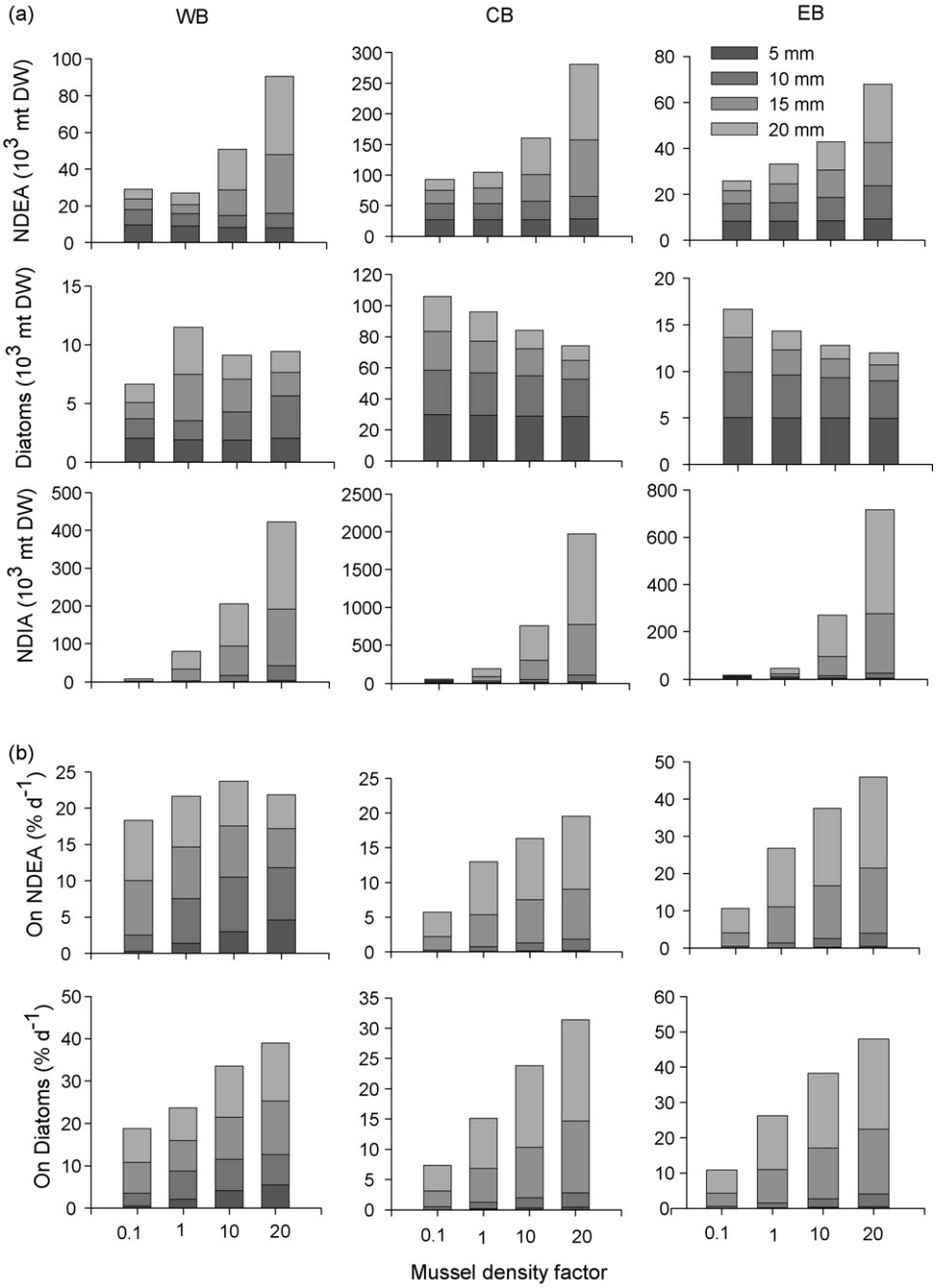

Fig. 11 – Uncertainty analysis of different combinations of density and body size of dreissenid mussel populations on (a) basin-wide algal biomass and (b) basin-wide grazing impacts of mussels. The values are averaged over the simulation period. Note the different scales on the *y*-axis.

monthly/seasonally averaged algal biomass between with and without mussels in the model system. For a complex ecosystem, it is hard to conclude that the observed differences are due only to mussels' grazing.

Our sensitivity analysis shows that a bigger dreissenid population (high density and/or large mussel sizes) will increase instead of decrease basin-wide NDEA biomass due to increased phosphorus excretion. Mellina et al. (1995) demonstrated this increase by measuring chlorophyll *a* in mesocosm (tank) experiments. NDEA are mainly small, rapidly growing species and have low sinking rates. Vanderploeg et al. (2001) also speculated that with increased nutrients excreted by mussels, NDEA should increase in growth faster than the mortality imposed by mussel grazing. Hence, these results suggest that dreissenid mussels play a more important role by recycling nutrients than they do by depressing algal biomass as population increases, especially in nutrient-limited, less productive water bodies.

Nicholls et al. (2002) reported that dreissenid mussels depress diatoms in lakes. Our simulation results indicate that

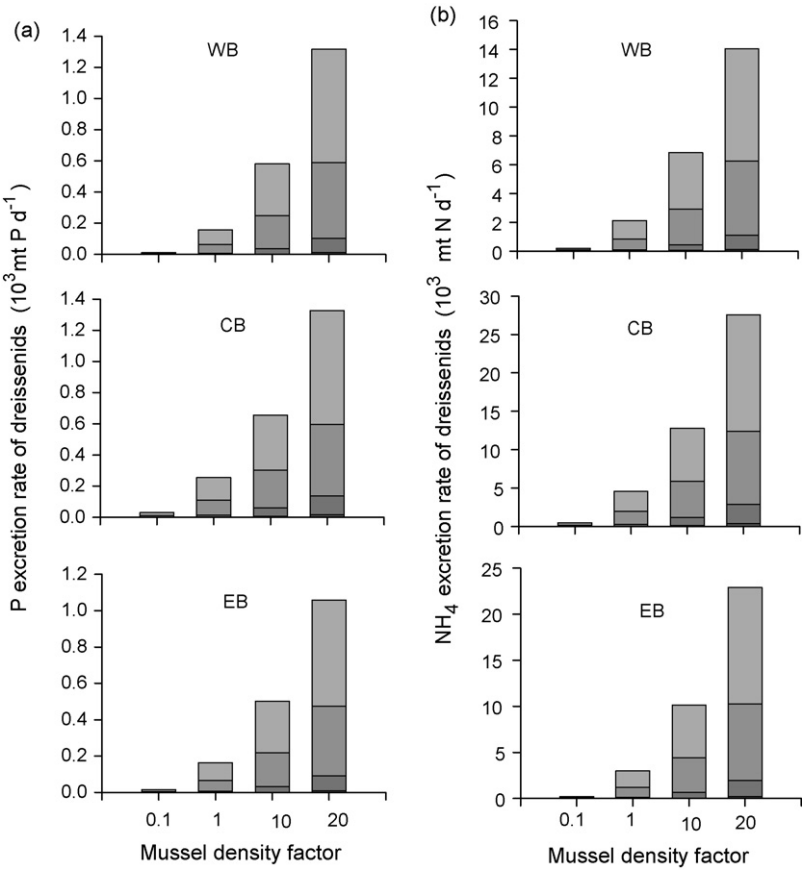

Fig. 12 – Uncertainty analysis of different combinations of density and body size of dreissenid mussel populations on basin-wide nutrient (P and N) excretion rates of dreissenid mussel populations. The values are averaged over the simulation period. See Fig. 11 for legends. Note the different scales on the y-axis.

the depression of diatoms may be attributed to their high sinking rates as well as their competition with NDEA.

NDIA are dominated by *Microcystis* in our model, so we will discuss *Microcystis* instead of NDIA below. *Microcystis* blooms have occurred with increased frequency and magnitude in Lake Erie since dreissenid mussels established large populations on the lake bottom. Vanderploeg et al. (2001) showed that zebra mussels selectively rejected toxic *Microcystis aeruginosa* in pseudofeces. Bierman et al. (2005) demonstrated the selective promotion of *Microcystis* by mussels in Saginaw Bay using a well-mixed water column model. The rising time and mechanism of dreissenid-rejected *Microcystis* transport from the bottom to the water column are still unclear. Our simulations show that *Microcystis* is not a strong nutrient competitor with other algal groups. When phosphorus concentration is low, *Microcystis* biomass decreases due to competition with other algae. However, *Microcystis* is less affected by the vertical distribution of P, but was more affected by the total amount of available P in the water column, because they require low light intensity (Hesse and Kohl, 2001) and can adjust their position in the water column by adjusting buoyancy (Brookes et al., 1998; Brookes and Ganf, 2001; Bonnet and Poulin, 2002). Thus, a high mussel population that excretes a large amount of phosphorus on the bottom will benefit *Microcystis* more than other algae, which is consistent with our finding that *Microcystis* has higher net productivity than NDEA in the western and eastern basins when the mussel population size is large.

However, our simulation results differ from those of Bierman et al. (2005) in several ways. First, their model consists of just one well-mixed layer, while ours has 2–65 layers depending on the depth of water in a given segment. Their assumption of a well-mixed water column may be appropriate for shallow Saginaw Bay, Lake Huron, but not for Lake Erie, even in the shallow western basin. As we have discussed earlier, their assumptions led to an overestimate of the dreissenid grazing impacts on algae other than *Microcystis*, which, in turn, enhanced the development of *Microcystis*. This is unlikely because *Microcystis* is not a strong competitor. Our results show that selective grazing by dreissenids showed little impact on the development of *Microcystis*, except in the western basin of 1998 when a *Microcystis* bloom occurred. Second, Bierman et al., did not separate the effects of dreissenid grazing on *Microcystis* from those of nutrient excretion when they tested the sensitivities of their model to variations in mussel densities. Our results clearly show that mussels have much stronger impacts on *Microcystis* by P excretion than by grazing, at least in Lake Erie.

Several studies have observed high algal biomass and production during recent years (Conroy et al., 2005b; Fitzpatrick

Table 7 – Statistical results of the uncertainties due to changing the simulated dreissenid population densities

State variables	Density factor of mussels	Means	Standard deviations	Paired t-test ($p < 0.05$)
NDEA (mg DW l^{-1})				
	1	0.178	0.199	a
	0.1	0.203	0.270	b
	10	0.174	0.150	a
NDIA				
	1	0.128	0.166	a
	0.1	0.134	0.173	b
	10	0.150	0.187	a
Diatoms				
	1	0.034	0.083	a
	0.1	0.018	0.030	b
	10	0.420	0.543	b
Copepods				
	1	0.037	0.029	a
	0.1	0.041	0.032	b
	10	0.040	0.037	a
Cladocerans				
	1	0.013	0.012	a
	0.1	0.016	0.014	b
	10	0.013	0.016	a
TP-F (mg P l^{-1})				
	1	0.005	0.003	a
	0.1	0.005	0.002	b
	10	0.010	0.011	b
NH_4 (mg N l^{-1})				
	1	0.017	0.009	a
	0.1	0.013	0.005	b
	10	0.070	0.098	b

Significant differences between density factor 1 and 0.1 or 1 and 10 are indicated by different letters in the last column.

et al., 2007). Some scientists speculated that these increases could result partially from increased light penetration in the water column accompanied by dreissenid mussels' colonization (Idrisi et al., 2001; Porta et al., 2005; Fitzpatrick et al., 2007). Our model uses Steele's (1962) equation to simulation light attenuation in the water column (see Section 2.2.3). Algal growth is limited by light during dawn and dusk and night. During these times, the light-limiting factor differed only around ±0.002 between with and without mussels. Charlton (2001) reported no significant difference in Secchi depth in the offshore area in the east and central basins between before and after mussel settlement, while in the western basin, the Secchi depth varied largely after mussel invasion. Barbiero and Tuchman (2004) found no evidence of persistent, basin-wide increases in water clarity in the western and central basins of Lake Erie in the post-dreissenid period and suggested that water clarity is largely affected by sediment loading and resuspension during periodic storms in the western basin.

In summary, our ecological model predictions show reasonable agreement with direct field observations, and allow us to determine that dreissenids decrease NDEA and diatom biomass by grazing while they increase NDEA and diatom biomass by nutrient excretion. Dreissenids cause NDIA to proliferate mainly by nutrient excretion instead of by selective rejection. Dreissenid mussels excrete large amounts of SRP and NH_3 to the nutrient pool. Mussel grazing impacts are depressed by stronger boundary layers, while nutrient excretion impacts become dominant with increasing mussel populations. As a result, NDEA and NDIA biomass increase with increasing mussel population to a high level. Diatom biomass decreases with large mussel population due to diatoms' higher sinking rates.

Acknowledgments

This study was sponsored by the Ohio Lake Erie Office—Lake Erie Protection Fund Project # LEPF 98-17, and the Ohio Department of Natural Resources as part of the Federal Aid in Sport Fish Restoration Program (F-69-P, Fish Management in Ohio) administered jointly by the U.S. Fish and Wildlife Service and the Ohio Division of Wildlife and the United States Environmental Protection Agency (GL-97590101), and NSF Environmental Biology Grant # DEB-0410336. We appreciate the valuable review comments from E.A. Marschall and R.M. Sykes at the Ohio State University. We thank two anonymous reviewers for helpful comments and suggestions on the manuscript. This is GLERL contribution No. 1461.

Appendix A

Kinetic parameters	Suggested range (Cole and Buchak, 1995)	Value used
Diatoms		
Growth rate (d^{-1})	1.1–2.0, 3.0[a]	3.0
Mortality rate (d^{-1})	0.01–0.1	0.07
Excretion rate (d^{-1})	0.01–0.04	0.01
Dark respiration rate (d^{-1})	0.02–0.04, 0.05[b]	0.05
Settling rate ($m\,d^{-1}$)	0.1–0.14, 0.8[c]	0.20
Algal half-saturation constant for ammonium ($g\,m^{-3}$)	0.014, 0.03[a]	0.03
Algal half-saturation constant for phosphorus ($g\,m^{-3}$)	0.003–0.009, 0.002[a]	0.002
Algal half-saturation constant for silica ($g\,m^{-3}$)	0.03[c]	0.03
Saturation intensity at maximum photosynthetic rate ($W\,m^{-2}$)	75–150	120
Silicon content of DW biomass ($g\,g\,DW^{-1}$)	0.21[d]	0.21
(1) Lower temperature for growth (°C)	4[d]	4
(2) Lower temperature for maximum growth (°C)	12[d]	12
(3) Upper temperature for maximum growth (°C)	16[d]	16
(4) Upper temperature for growth (°C)	35[b]	35
Fraction of algal growth rate at (1)	0.10	0.10
Fraction of algal growth rate at (2)	0.99	0.99
Fraction of algal growth rate at (3)	0.99	0.99
Fraction of algal growth rate at (4)	0.10	0.10
NDEA		
Growth rate (d^{-1})	1.1–2.0, 3.0[a]	3.0
Mortality rate (d^{-1})	0.01–0.1	0.07
Excretion rate (d^{-1})	0.01–0.04	0.01
Dark respiration rate (d^{-1})	0.02–0.04, 0.05[b]	0.05
Settling rate ($m\,d^{-1}$)	0.1–0.14, 0.05[c]	0.05
Algal half-saturation constant for ammonium ($g\,m^{-3}$)	0.014, 0.03[b]	0.03
Algal half-saturation constant for phosphorus ($g\,m^{-3}$)	0.003–0.009, 0.002[a]	0.002
Saturation intensity at maximum photosynthetic rate ($W\,m^{-2}$)	75–150	120
(5) Lower temperature for growth (°C)	4[d]	4
(6) Lower temperature for maximum growth (°C)	18[d]	18
(7) Upper temperature for maximum growth (°C)	25[d]	25
(8) Upper temperature for growth (°C)	35[b]	35
Fraction of algal growth rate at (5)	0.10	0.10
Fraction of algal growth rate at (6)	0.99	0.99
Fraction of algal growth rate at (7)	0.99	0.99
Fraction of algal growth rate at (8)	0.10	0.10
NDIA		
Growth rate (d^{-1})	1.1–2.0	2.0
Mortality rate (d^{-1})	0.01–0.1	0.03
Excretion rate (d^{-1})	0.01–0.04	0.04
Dark respiration rate (d^{-1})	0.02–0.04, 0.05[b]	0.05
Settling rate ($m\,d^{-1}$)	0.1–0.14, 0.05[c]	0.05
Algal half-saturation constant for ammonium ($g\,m^{-3}$)	0.001[d]	0.001
Algal half-saturation constant for phosphorus ($g\,m^{-3}$)	0.010[b]	0.010
Saturation intensity at maximum photosynthetic rate ($W\,m^{-2}$)	50[a]	50
(9) Lower temperature for growth (°C)	15[d]	15
(10) Lower temperature for maximum growth (°C)	22[d]	22
(11) Upper temperature for maximum growth (°C)	30[b]	30
(12) Upper temperature for growth (°C)	35[b]	35
Fraction of algal growth rate at (9)	0.10	0.10
Fraction of algal growth rate at (10)	0.99	0.99

Appendix A (*Continued*)

Kinetic parameters	Suggested range (Cole and Buchak, 1995)	Value used
Fraction of algal growth rate at (11)	0.99	0.99
Fraction of algal growth rate at (12)	0.10	0.10
Fraction of algal biomass lost by mortality to detritus	0.8	0.8
Labile dissolved organic material decay rate (d^{-1})	0.12	0.12
Detritus decay rate (d^{-1})	0.06–0.08	0.08
Detritus settling rate ($m\,d^{-1}$)	0.35–0.5	0.5
Diatom detritus decay rate (d^{-1})	0.08[d]	0.08
Diatom detritus settling rate ($m\,d^{-1}$)	0.8[d]	0.8
(13) lower temperature for organic matter decay (°C)	4–5	5.0
(14) Lower temperature for maximum organic matter decay (°C)	20–25	25
Fraction of organic matter decay rate at (13)	0.10	0.10
Fraction of organic matter decay rate at (14)	0.99	0.99
Maximum sediment oxygen demand ($g\,O_2\,m^{-2}\,d^{-1}$)	0.1–0.27[e,f,g], 1.6–3.9[h]	0.22
Oxygen half-saturation constant for SOD ($g\,O_2\,m^{-3}$)	1.4[g]	1.4
Temperature coefficient, θ	1.047–1.0147	1.047
Anaerobic sediment release rate of phosphorus ($g\,m^{-2}\,d^{-1}$)	0.015–0.3, 0.001–0.002[a]	0.002
Anaerobic release rate of ammonium ($g\,m^{-2}\,d^{-1}$)	0.05–0.4, 0.004–0.01[a]	0.005
Ammonium decay rate (oxidation to nitrate) (d^{-1})	0.12	0.12
(15) Lower temperature for ammonium decay (°C)	5	5.0
(16) Lower temperature for maximum ammonium decay (°C)	20–25	25
Fraction of nitrification rate at (15)	0.10	0.10
Fraction of nitrification rate at (16)	0.99	0.99
Nitrate decay rate (d^{-1})	0.05–0.15	0.05
(17) Lower temperature for nitrate decay (°C)	5	5.0
(18) Lower temperature for maximum nitrate decay (°C)	20–25	25
Fraction of denitrification rate at (17)	0.10	0.10
Fraction of denitrification rate at (18)	0.99	0.99
Oxygen stoichiometric equivalent for ammonium decay	4.57	4.57
Oxygen stoichiometric equivalent for organic matter decay	1.4	1.4
Oxygen stoichiometric equivalent for algal growth	1.4	1.4
Stoichiometric equivalent between organic matter and phosphorus	0.005–0.011	0.01
Stoichiometric equivalent between organic matter and nitrogen	0.08	0.08
Stoichiometric equivalent between organic matter and carbon	0.45	0.45
Dissolved oxygen concentration at which anaerobic processes begin ($g\,m^{-3}$)	0.05–0.1	0.1

[a] Bowie et al. (1985 and references therein).
[b] Scavia (1980).
[c] Scavia et al. (1988).
[d] This study.
[e] Di Toro and Connolly (1980).
[f] Lam et al. (1983).
[g] Lam et al. (1987).
[h] Lucas and Thomas (1972).

Appendix B

Equations of cladocerans

$\frac{dZ}{dt} = (Ag - r - s)Z - P$, where
A is assimilation rate
g is ingestion rate $g = g_{max}\frac{F}{K+F}$
g_{max} is the maximal weight-specific ingestion rate, K is the half-saturation constant, F is the weighted combination of algae and detritus
r is respiration loss, which consists of a basic value and a portion that proportional to the food function. i.e. $r = \left(r_1 + r_2\frac{F}{K+F}\right)\theta^{(T-20)}$
s is the loss of starvation, $s = s_0 \min\left(1, 1 - \frac{g}{g_s}\right)$,
P is the predation loss. $P = p_0\left(\frac{Z}{Z_h+Z}\right)Z$

Parameter definitions and estimates for cladoceran submodel	Sources	Used
Maximum consumption rate, g_{max} (d^{-1})	0.8–1.6[a]	0.8–1.0
Basic respiration rate, r_1 (d^{-1})	0.1[a]	0.1
Food dependent respiration rate, r_2 (d^{-1})	0.25[a]	0.25
Assimilation rate, A	0.5–0.7[a]	0.6
Half-saturation food constant, K ($g\,C\,m^{-3}$)	0.18[a]	0.16
Maximum starvation loss rate, s_0 (d^{-1})	0.3[b]	0.3
Minimum non-starving consumption rate, g_s (d^{-1})	0.05[b]	0.05
Maximum predation loss rate, P_0 (d^{-1})	0.8[b]	0.8
Half-saturation predation constant, Z_h ($g\,DW\,m^{-3}$)	0.5[b]	0.5

[a] Scavia et al. (1988).
[b] This study.

REFERENCES

Ackerman, J.D., Loewen, M.R., Hamblin, P.F., 2001. Benthic-Pelagic coupling over a zebra mussel reef in western Lake Erie. Limnol. Oceanogr. 46, 892–904.

Arnott, D.L., Vanni, M.J., 1996. Nitrogen and phosphorus recycling by the zebra mussel (*Dreissena polymorpha*) in the western basin of Lake Erie. Can. J. Fish. Aquat. Sci. 53, 646–659.

Baldwin, B.S., Mayer, M.S., Dayton, J., Pau, N., Mendilla, J., Sullivan, M., Moore, A., Ma, A., Mills, E.L., 2002. Comparative growth and feeding in zebra and quagga mussels (*Dreissena polymorpha* and *Dreissena bugensis*): implications for North American lakes. Can. J. Fish. Aquat. Sci. 59, 680–694.

Barbiero, R.P., Tuchman, M.L., 2004. Long-term dreissenid impacts on water clarity in Lake Erie. J. Great Lakes Res. 30, 557–565.

Bertram, P.E., 1993. Total phosphorus and dissolved oxygen trends in the central basin of Lake Erie, 1970–1991. J. Great Lakes Res. 19, 224–236.

Bierman, V.J., Kaur, J., DePinto, J.V., Feist, T.J., Dilks, D.W., 2005. Modeling the role of zebra mussels in the proliferation of blue-green algae in Saginaw Bay, Lake Huron. J. Great Lakes Res. 31, 32–55.

Boegman, L., Loewen, M.R., Hamblin, P.F., Culver, D.A., 2001. Application of a two-dimensional hydrodynamic reservoir model to Lake Erie. Can. J. Fish. Aquat. Sci. 58, 858–869.

Boegman, L., Loewen, M.R., Hamblin, P.F., Culver, D.A., 2008a. Vertical mixing and weak stratification over zebra mussel colonies in western Lake Erie. Limnol. Oceanogr. 53, 1093–1110.

Boegman, L., Loewen, M.R., Culver, D.A., Hamblin, P.F., Charlton, M.N., 2008b. Spatial-dynamic modeling of lower trophic levels in Lake Erie: Relative impacts of dreissenid mussels and nutrient loads. J. Environ. Eng.-ASCE 134.

Bonnet, M.P., Poulin, M., 2002. Numerical modeling of the planktonic succession in a nutrient-rich reservoir: environmental and physiological factors leading to *Microcystis aeruginosa* dominance. Ecol. Model. 156, 93–112.

Bowie, G.L., Mills, W.B., Porcella, D.B., Campbell, C.L., Pagenkopf, J.R., Rupp, G.L., Johnson, K.M., Chan, P.W.H., Gherini, S.A., 1985. Rates, Constants, and Kinetics Formulations in Surface Water Quality Modeling. U.S. Environmental Protection Agency, Environmental Research Laboratory, Athens, Georgia (EPA/600/3-85/040).

Bridgeman, T.B., Schloesser, D.W., Krause, A.E., 2006. Recruitment of *Hexagenia* mayfly nymphs in western Lake Erie linked to environmental variability. Ecol. Appl. 16 (2), 601–611.

Brookes, J.D., Ganf, G.G., 2001. Variations in the buoyancy response of *Microcystis aeruginosa* to nitrogen, phosphorus and light. J. Plank. Res. 23, 1399–1411.

Brookes, J.D., Ganf, G.G., Burch, M.D., 1998. Buoyancy regulation of *Microcystis aeruginosa*. Verh. Internat. Verein. Limnol. 26, 1670–1673.

Bunt, C.M., MacIsaac, H.J., Sprules, W.G., 1993. Pumping rates and projected filtering impacts of juvenile zebra mussels (*Dreissena polymorpha*) in the western Lake Erie. Can. J. Fish. Aquat. Sci. 50, 1017–1022.

Chapra, S.C., 1979. Application of the phosphorus loading concept to the Great Lakes. In: Loehr, R.C., Martin, C.S., Rast, W. (Eds.), Phosphorus Management Strategies for Lakes: Proceedings of the 1979 Conference. New York, pp. 135–152.

Charlton, M.N., 2001. Did zebra mussels clean up Lake Erie? Great Lakes Res. Rev. 5, 11–15.

Cole, T.M., Buchak, E.M., 1995. CE-QUAL-W2: a two-dimensional, laterally averaged, hydrodynamic and water quality model, version 2.0: User manual. Instruction Report EL-95-1, US Army Corps of Engineers, Washington, DC 20314-1000.

Cole, T.M., Wells, S.A., 2003. CE-QUAL-W2: a two-dimensional, laterally averaged, hydrodynamic and water quality model, version 3.1: User manual. Instruction Report EL-03-1, US Army Corps of Engineers, Washington, DC 20314-1000.

Conroy, J.D., Culver, D.A., 2005. Do dreissenids affect Lake Erie ecosystem stability processes? Am. Midl. Nat. 153, 20–32.

Conroy, J.D., Edwards, W.J., Pontius, R.A., Kane, D.D., Zhang, H., Shea, J.F., Richey, J.N., Culver, D.A., 2005a. Soluble nitrogen and phosphorus excretion of exotic freshwater mussels (*Dreissena* spp.): potential impacts for nutrient remineralization in western Lake Erie. Freshwater Biol. 50, 1146–1162.

Conroy, J.D., Kane, D.D., Dolan, D.M., Edwards, W.J., Charlton, M.N., Culver, D.A., 2005b. Temporal trends in Lake Erie plankton biomass: roles of external phosphorus loading and dreissenid mussels. J. Great Lakes Res. 31 (Suppl. 2), 89–110.

Di Toro, D.M., 1983. Documentation for Water Quality Analysis Simulation Program (WASP) and Model Verification Program (MVP). For USEPA, Duluth, MN (68-01-3872).

Di Toro, D.M., Connolly, J.P., 1980. Mathematical models of water quality in large lakes. Part 2: Lake Erie. USEPA, Office of

Research and Development, ERL-Duluth, LLRS, Grosse Ile, MI. EPA Ecological Research Series EPA-600/3-80-065.
Edwards, W.J., 2002. Impacts of the zebra mussel (*Dreissena polymorpha*) on large lakes: influence of vertical turbulent mixing. Ph.D. Dissertation, Department of Evolution, Ecology, and Organismal Biology, The Ohio State University, Columbus, OH.
Edwards, W.J., Rehmann, C.R., McDonald, E., Culver, D.A., 2005. The impact of a benthic filter feeder: limitations imposed by physical transport of algae to the benthos. Can. J. Fish. Aquat. Sci. 62, 205–214.
Fanslow, D.L., Nalepa, T.F., Lang, G.A., 1995. Filtration rates of the zebra mussel (*Dreissena polymorpha*) on natural seston from Saginaw Bay, Lake Huron. J. Great Lakes Res. 21, 489–500.
Fennel, W., Neumann, T., 2003. Variability of copepods as seen in a coupled physical-biological model of the Baltic Sea. In: ICES Marine Science Symposia, 219, pp. 208–219.
Fitzpatrick, M.A.J., Munawar, M., Leach, J.H., Haffner, G.D., 2007. Factors regulating primary production and phytoplankton dynamics in western Lake Erie. Fund. Appl. Limnol. 169 (2), 137–152.
Gopalan, G., Culver, D.A., Wu, L., Trauben, B.K., 1998. Effects of recent ecosystem changes on the recruitment of young-of-the-year fish in western Lake Erie. Can. J. Fish. Aquat. Sci. 55, 2572–2579.
Hartley, R.P., Potos, C.P., 1971. Algal–Temperature–Nutrient Relationships and Distribution in Lake Erie. US Environment Protection Agency, Water Quality Office, Region V, Lake Erie Basin (February).
Hesse, K., Kohl, J.-G., 2001. Effect of light and nutrient supply on growth and microcystin content of different strains of *Microcystis aeruginosa*. In: Chorus, I. (Ed.), Cyanotoxins—Occurrence, Causes, Consequences. Springer-Verlag, Berlin/Heidelberg, Germany, pp. 104–115.
Holland, R.E., 1993. Changes in planktonic diatoms and water transparency in Hatchery Bay, Bass Island area, western Lake Erie since the establishment of the zebra mussel. J. Great Lakes Res. 19, 717–724.
Horgan, M.J., Mills, E.L., 1997. Clearance rates and filtering activity of zebra mussel (*Dreissena polymorpha*): implications for freshwater lakes. Can. J. Fish. Aquat. Sci. 54, 249–255.
Idrisi, N., Mills, E.L., Rudstam, L.G., Stewart, D.J., 2001. Impact of zebra mussels (*Dreissena polymorpha*) on the pelagic lower trophic levels of Oneida Lake, New York. Can. J. Fish. Aquat. Sci. 58, 1430–1441.
Jarvis, P., Dow, J., Dermott, R., Bonnell, R., 2000. Zebra (*Dreissena polymorpha*) and quagga mussel (*Dreissena bugensis*) distribution and density in Lake Erie, 1992–1998. Can. Tech. Rep. Fish. Aquat. Sci. 2304, 46.
Krieger, K.A., Schloesser, D.W., Manny, B.A., Trisler, C.E., Heady, S.E., Ciborowski, J.J.H., Muth, K.M., 1996. Recovery of burrowing mayflies (Ephemeroptera: Ephemeridae: *Hexagenia*) in western Lake Erie. J. Great Lakes Res. 22, 254–263.
Krondratev, G.P., 1963. O nekotoryh osobennostjah filtracii u presnovodnyh molljuskov. Nauncnye doklady vyssej skoly Biol Nauki (Moskow) 1, 13–16.
Kryger, J., Riisgard, H.U., 1988. Filtration rate capacities in 6 species of European freshwater bivalves. Oecologia 77, 34–38.
Lam, D.C., Schertzer, W.M., Fraser, A.S., 1983. Simulation of Lake Erie Water Quality Responses to Loading and Weather Variations. National Water Research Institute, Inland Waters Directorate, Canada Center for Inland Waters, Burlington, Ontario (Scientific series No. 134).
Lam, D.C., Schertzer, W.M., Fraser, A.S., 1987. Oxygen depletion in Lake Erie: modeling the physical, chemical, and biological interactions, 1972 and 1979. J. Great Lakes Res. 13, 770–781.
Leach, J.H., 1993. Impacts of the zebra mussel (*Dreissena polymorpha*) on water quality and fish spawning reefs in western Lake Erie. In: Nalepa, T.F., Schloesser, D.W. (Eds.), Zebra Mussels: Biology, Impacts, and Control. Lewis Publishers/CRC press, Boca Raton, FL, pp. 381–397.
Leon, L.F., Smith, R.E.H., Romero, J.R., Hecky, R.E., 2006. Lake Erie hypoxia simulations with ELCOM-CAEDYM. In: Proceedings of the 3rd Biennial meeting of the International Environmental Modelling and Software Society, Burlington, Vermont, July 9–13.
Loewen, M.R., Ackerman, J.D., Hamblin, P.F., 2007. Environmental implications of stratification and turbulent mixing in a shallow lake basin. Can. J. Fish. Aquat. Sci 64, 43–57.
Lucas, A.M., Thomas, N.A., 1972. Sediment oxygen demand in Lake Erie's Central basin, 1970. In: Burns, N.M., Ross, C. (Eds.), Project Hypo—an intensive study of the Lake Erie central basin hypolimnion and related surface water phenomena. Canada Centre for Inland Waters, Paper No. 6. United States Environmental Protection Agency, Technical Report, TS-05-71-208-24. February 1972, pp. 45–50.
MacIsaac, H.J., Sprules, G.W., Leach, J.H., 1991. Ingestion of small-bodied zooplankton by zebra mussels (*Dreissena polymorpha*): can cannibalism on larvae influence population dynamics? Can. J. Fish. Aquat. Sci. 48, 2051–2060.
MacIsaac, H.J., Sprules, W.G., Johannsson, O.E., Leach, J.H., 1992. Filtering impacts of larval and sessile zebra mussels (*Dreissena polymorpha*) in western Lake Erie. Oecologia 92, 30–39.
MacIsaac, H.J., Lonnee, C.J., Leach, J.H., 1995. Suppression of microzooplankton by zebra mussels: importance of mussel size. Freshwater Biol. 34, 379–387.
MacIsaac, H.J., Johannsson, O.E., Ye, J., Sprules, W.G., Leach, J.H., McCorquodale, J.A., Grigorovich, I.A., 1999. Filtering impacts of an introduced bivalve (*Dreissena polymorpha*) in a shallow lake: application of hydrodynamic model. Ecosystems 2, 338–350.
Makarewicz, J.C., Bertram, P., 1991. Evidence for the restoration of the Lake Erie North America ecosystem: water quality oxygen levels and pelagic function appear to be improving. Bioscience 41, 216–223.
May, B., Marsden, J.E., 1992. Genetic identification and implications of another invasive species of dreissenid mussel in the Great Lakes. Can. J. Fish. Aquat. Sci. 49, 1501–1506.
McCune, K.C., 1998. Temperature gradient microprofiling in the central basin of Lake Erie: a study of vertical turbulent processes. M.S. Thesis. The Ohio State University.
Mellina, E., Rasmussen, J.B., Mills, E.L., 1995. Impact of zebra mussel (*Dreissena polymorpha*) on phosphorus cycling and chlorophyll in lakes. Can. J. Fish. Aquat. Sci. 52, 2553–2573.
Micheev, V.P., 1966. O skorosti fil tracii vody Drejessenoj. Tr. Inst. Biol. Vodokhran Akad Nauk SSSR 12, 134–138.
Mills, E.L., Chrisman, J.R., Baldwin, B.S., Howell, T., Owens, R.W., O'Gorman, R., Roseman, E.F., Raths, M.K., 1999. Changes in the dreissenid community and a shift toward dominance of the quagga mussel (*Dreissena bugensis*) in the lower Great Lakes. J. Great Lakes Res. 25, 187–197.
Nicholls, K.H., Heintsch, L., Carney, E., 2002. Univariate step-trend and multivariate assessments of the apparent effects of P loading reductions and zebra mussels on the phytoplankton of the Bay of Quinte, Lake Ontario. J. Great Lakes Res. 28, 15–31.
Noonburg, E.G., Shuter, B.J., Abrams, P.A., 2003. Indirect effects of zebra mussels (*Dreissena polymorpha*) on the planktonic food web. Can. J. Fish. Aquat. Sci. 60, 1353–1368.
Palmieri, V., de Carvalho, R.J., 2006. Qual2e model for the Corumbataí River. Ecol. Model. 198, 269–275.
Pontius, R.A., 2000. The impact of zebra mussels (*Dreissena polymorpha*) on pelagic food webs. Ph.D. Dissertation, Department of Evolution, Ecology, and Organismal Biology, The Ohio State University, Columbus, OH.

Porta, D., Fitzpatrick, M.A.J., Haffner, G.D., 2005. Annual variability of phytoplankton primary production in the Western Basin of Lake Erie (2002–2003). J. Great Lakes Res. 31 (Suppl. 2), 63–71.

Rinta-Kanto, I.M., Ouellette, A.J.A., Boyer, G.L., Twiss, M.R., Bridgeman, T.B., Wilhelm, S.W., 2005. Quantification of toxic *Microcystis* spp. during the 2003 and 2004 blooms in western Lake Erie using quantitative real-time PCR. Environ. Sci. Technol. 39, 4198–4205.

Rockwell, D.C., Salisbury, D.K., Lesht, B.M., 1989. Water quality in the middle Great Lakes: results of the 1985 USEPA survey of lakes Erie, Huron and Michigan. Rep. No. EPA 605/6-89-001. U.S. Environmental Protection Agency, Great Lakes National Program Office. 230 South Dearborn, Chicago, IL 60604.

Roe, S.L., MacIsaac, H.J., 1997. Deepwater population structure and reproductive state of quagga mussels (*Dreissena bugensis*) in Lake Erie. Can. J. Fish. Aquat. Sci. 54, 2428–2433.

Scavia, D., 1980. An ecological model of Lake Ontario. Ecol. Model. 8, 49–78.

Scavia, D., Lang, G.A., Kitchell, J.F., 1988. Dynamics of Lake Michigan plankton: a model evaluation of nutrient loading, competition, and predation. Can. J. Fish. Aquat. Sci. 45, 165–177.

Schertzer, W.M., Saylor, J.H., Boyce, F.M., Robertson, D.G., Rosa, F., 1987. Seasonal thermal cycle of Lake Erie. J. Great Lakes Res. 13, 468–486.

Steele, J.H., 1962. Environmental control of photosynthesis in the sea. Limnol. Oceanogr. 7, 137–150.

Stoeckmann, A., 2003. Physiological energetics of Lake Erie dreissenid mussels: a basis for the displacement of *Dreissena polymorpha* by *Dreissena bugensis*. Can. J. Fish. Aquat. Sci. 60, 126–134.

Talling, J.F., 2003. Phytoplankton-zooplankton seasonal timing and the 'clear-water phase' in some English lakes. Freshwater Biol. 48, 39–52.

Thornton, K.W., Lessem, A.S., 1978. A temperature algorithm for modifying biological rates. Trans. Am. Fish. Soc. 107, 284–287.

Vanderploeg, H.A., Liebig, J.R., Carmichael, W.W., Age, M.A., Johengen, T.H., Fahnenstiel, G.L., Nalepa, T.F., 2001. Zebra mussel (*Dreissena polymorpha*) selective filtration promoted toxic *Microcystis* blooms in Saginaw Bay (Lake Huron) and Lake Erie. Can. J. Fish. Aquat. Sci. 58, 1208–1221.

Vincent, R.K., Qin, X., McKay, R.M.L., Miner, J., Czajkowski, K., Savino, J., Bridgeman, T., 2004. Phycocyanin detection from LANDSAT TM data for mapping cyanobacterial blooms in Lake Erie. Remote Sens. Environ. 89, 381–392.

Vollenweider, R.A., Rast, W., Kerekes, J., 1979. The phosphorus loading concept and Great Lakes eutrophication. In: Loehr, R.C., Martin, C.S., Rast, W. (Eds.), Phosphorus Management Strategies for Lakes: Proceedings of the 1979 Conference. New York, pp. 207–234.

Wu, L., Culver, D.A., 1991. Zooplankton grazing and phytoplankton abundance an assessment before and after invasion of *Dreissena polymorpha*. J. Great Lakes Res. 17, 425–436.

Wu, L., Culver, D.A., 1994. *Daphnia* population-dynamics in western Lake Erie—regulation by food limitation and yellow perch predation. J. Great Lakes Res. 20, 537–545.

Zhang, H., 2006. Ecological modeling of the lower trophic levels of Lake Erie. Ph.D. Dissertation, the Department of Evolution, Ecology and Organismal Biology, The Ohio State University, Columbus, OH.